Characterization of a TAXI-TRAP Substrate-Binding Protein from *Vibrio cholerae*

Nicholas Daniel Massouh

KENT ID: 20902727

Thesis submitted to the School of Biosciences, University of Kent

MSc-R in Biochemistry

2021

Supervisor: Christopher Mulligan

Word Count: 16,261

Declaration

No part of this thesis has been submitted in support of an application for any degree or qualification of the University of Kent or any other University or Institute of learning.

Signature: Nicholas Massouh

Date: October 2021

Acknowledgements

The research summarized throughout this thesis would not have been possible without the network of people I have had around me during my degree. Hence, I would like to show my appreciation to all those who have supported me.

Firstly, I would like to thank Dr. Chris Mulligan for his teaching, guidance, and overall enthusiastic approach to my learning throughout the past year. I would also like to thank all members of both Robinson lab and Mulligan lab for their support; with special mention going to Bree Streather and Matt Batson, who have made my time in the lab both interesting and entertaining.

Furthermore, I give my gratitude and appreciation to all my amazing friends in Canterbury, with specific mention to my housemates Kamal Fruci-Oduah and Beth Ellis. I also want to thank my brothers Aleksander Wiltshire and Jason Kufakwaro for always believing in me. A special mention goes to Roshan Sathiakeery- I would not be at this stage in my education without his support.

I want to thank my partner Nina for her love and patience and finally, I thank my family (with specific mention to my mum) for their love and support throughout.

Abbreviations

Amp	Ampicillin
CCCP	Carbonyl cyanide m-chlorophenyl hydrazone
DTT	Dithiothreitol
FT	Flow-through
GMQE	Global model quality estimate
IM	Inner membrane
IPTG	Isopropylthio-β-galactoside
IMAC	Immobilized metal affinity chromatography
LPS	Lipopolysaccharide
LB	Lysogeny broth
LBab	Lysogeny broth + antibiotic
MST	Microscale thermophoresis
MDH	Malate dehydrogenase
MSG	Monosodium glutamate
Ni-NTA	Nickel-chelating nitrilotriacetic acid
Kav	Partition coefficient
SBP	Substrate-binding protein
SOC	Super optimal broth with catabolite repression
SDM	Site-directed mutagenesis
SEC	Size exclusion chromatography
TTT	Tripartite tricarboxylate transporter
TRAP	Tripartite-ATP-independent periplasmic
TPR	Tetratricopeptide motif-protein
TPAT	Tetratricopeptide motif-protein (TPR) associated transporter
TEMED	Tetramethylethylenediamine
WB	Wash buffer

Abstract

TAXI-TRAP transporters represent a class of secondary substrate-binding protein (SBP)-dependent systems that are utilized by certain bacteria for the high affinity uptake and transport of substrates across the membrane. A limited number of studies have provided evidence of the substrate range of some TAXI-TRAP SBPs, but a full biochemical characterization of one of these essential components of a TAXI-TRAP system is still absent from literature.

In this study, we characterize a SBP, VC0430, from a TAXI-TRAP system that was identified in the facultative pathogen, *Vibrio cholerae*. Analysis of genes that are within the same genetic neighbourhood as *vc0430* suggested a function of the protein in the transport of carboxylic acids across the membrane. We capitalized on this clue by generating an accurate homology model of VC0430 and then mapped its binding site against the only TAXI-TRAP SBP crystal structure that is available in literature. Along with the insight provided by a multiple sequence alignment between the two proteins, this binding site superimposition enabled us to identify conserved residues in VC0430 that are involved in the binding of glutamate and glutamine. We proved this predicted substrate range to be correct through the use of thermal shift assays, whereby glutamate and glutamine were the only substrates to increase the thermal stability of the protein.

Lastly, having proven that VC0430 is a glutamate/glutamine binding protein, we speculated the significance of these two substrates to *Vibrio cholerae* and suggested the part that VC0430 could play in the survival of the bacterium. As glutamate, and hence glutamine as its metabolic precursor, has an important role in the osmoadaptation of *Vibrio cholerae* to both the estuarine and human intestinal environment, we identify VC0430 as a potential drug target to combat disease caused by this pathogen. We also provide experimental methods that can help further characterize the TAXI-TRAP family in future studies.

CONTENTS

LIST OF FIGURES

LIST OF TABLES

CHAPTER 1: INTRODUCTION

1.1. Background

Substrate-binding protein (SBP)-dependent transporters provide a high-affinity uptake system which is crucial for the survival of various types of prokaryotic organisms in their respective environments. SBPs, the extracytoplasmic domains of SBP-dependent transporters, are responsible for foraging essential nutrients so that they may be subsequently transported across the membrane by the transmembrane domain of the transporter [1]. The unique ability of these transporters to scavenge substrates at high-affinities using an extracytoplasmic component sets them apart from single-protein uptake systems, whilst also providing a valuable target for the development of membrane transporter inhibitors [2]. Transporters of this kind are categorized into two different subtypes; primary transporters which make use of external energy sources to fuel transport, such as the ATP-binding cassette (ABC) family [3], or ATP-independent secondary transporters which are powered by electrochemical ion gradients.

Secondary SBP-dependent transporters exist in two different subcategories; the tripartite tricarboxylate transporter family (TTT) and the tripartite-ATP-independent periplasmic (TRAP) transporter family [4]. Despite a lack of sequence similarity between these two families of transporter, both systems share a 'tripartite nature' in the sense that they are comprised of three domains [5]; a well conserved transmembrane helix protein (usually consisting of 12 subunits) that is thought to be responsible for the movement of substrates across the cytoplasmic membrane, a poorly conserved 4-transmembrane helix protein that is essential for TRAP transporters but has unknown function, and an extramembrane SBP [4].

Despite some increased momentum in the last two decades, TTT and TRAP transporters are still significantly less well-understood compared to their primary transporter counterparts. Nevertheless, most of the current literature centred around these transporters has targeted the periplasmic SBPs in these systems, with there now being a growing library of SBPs that have been both crystalized and biochemically characterized for each subcategory of secondary SBP-dependent transporter. As is the case with SBPs from other families, TTT and TRAP transporter SBPs have been shown to share the characteristic bilobular 'Venus fly-trap' tertiary composition [6]; consisting of a α-helical backbone that links together the two β-sheet-composed lobes (see Fig. 1) [7]. In their unbound form, SBPs from some ABC systems have been shown to loiter in their open-state (Fig. 1A) [8–10], which is not recognised by the transmembrane domains of the transporter. It is only upon ligand binding, and a subsequent shift to the closed-state, that the SBP becomes recognisable to the transmembrane domains

(Fig. 1B) and thus able to bequeath its substrate so that it may be translocated (Fig. 1 C-D) [11]. The existence of this same transport mechanism in VcSiaP, a well characterized SBP from the TRAP transporter family, has been implied in a recent FRET-based study [6], suggesting that this process could be synonymous amongst SBPs in TTT and TRAP systems.

Once more SBPs from these two secondary systems and their subgroups (see 1.2 & 1.3) have been characterized, and their respective substrates identified, more meticulous analysis on their transport mechanisms can be performed. Considering many TTT and TRAP transporters are potential targets for the development of inhibitors (for example TctC [7] and STM3169 [12], SBPs from the TTT and TRAP families, respectively, in *S. typhimurium*) it is of great value that biochemical characterization and identification of substrate specificity for these transporters is determined. This is what we aim to demonstrate for the poorly described TAXI (TRAP associated extracytoplasmic immunogenic)-TRAP subgroup of TRAP transporters (see 1.3.2.) in this project.

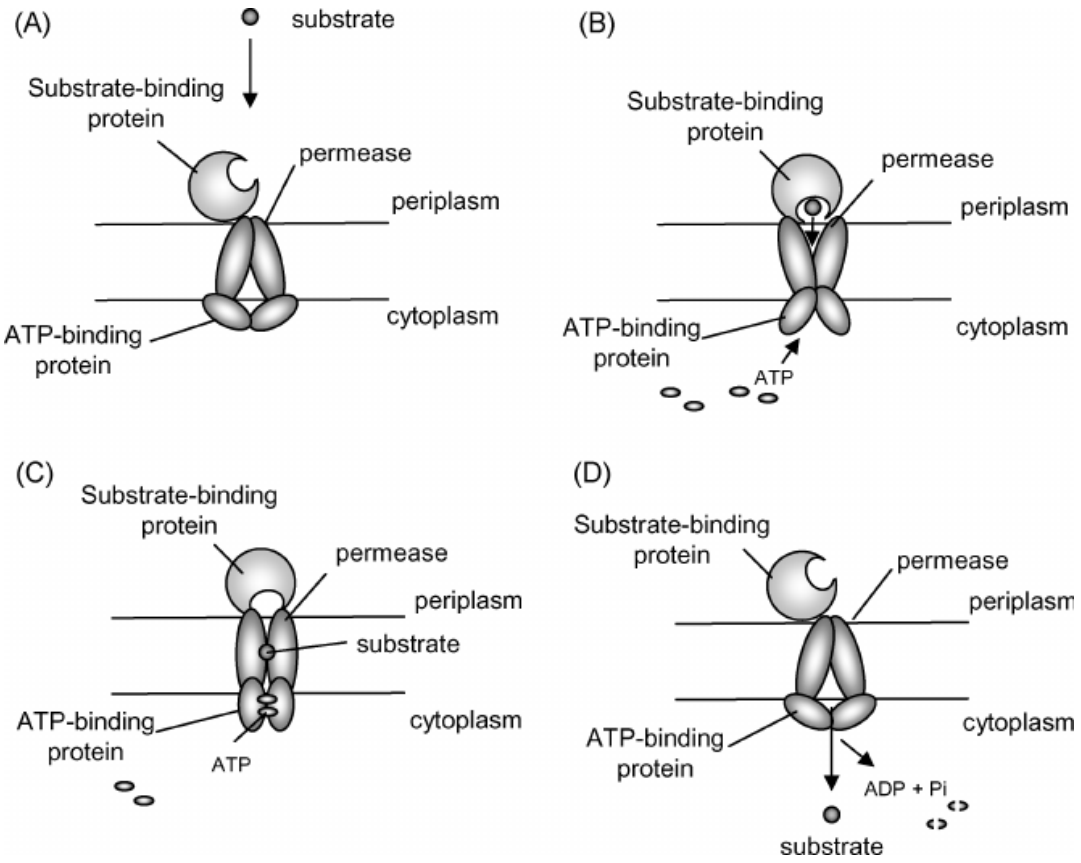

Figure 1. Typical structure and mechanism of an ABC transporter. (A) This illustration represents the general structure of an ABC system in Gram-positive bacteria. It is comprised of an unbound SBP that is tethered to either the periplasm or transmembrane domains, two membrane bound permeases which form the transmembrane domains, and an ATP-binding domain on surface of the cytoplasm. (B) Once the SBP captures its substrate, it moves to face towards the transmembrane domains. Simultaneously, ATP binds to the ATP-binding domain. (C) The transmembrane and ATP-binding domains change conformation to create a translocation pathway, and the substrate is then released by the SBP. (D) The substrate moves along the translocation pathway before reaching the ATP-binding domains, where it is then released into the cytoplasm as ATP is hydrolyzed. Figure taken from [13].

1.2. The TTT Family

Constituents of the TTT family of secondary transporters are primarily found in bacteria and are rarely present within archaea [5]. Despite having a very similar topology and function to TRAP transporters, the two systems share very little sequence similarity and have thus been categorised into two distinct families. The founding member of the TTT family, TctABC from *S. typhimurium*, was first discovered by Sweet *et al.* in their study of the periplasmic component, TctC, and its substrates [14]. Deletion of the TctC gene from the organism resulted in reduction of its ability to uptake citrate along with some of its homologues, such as isocitrate and fluorocitrate, however it was only after subsequent research that a larger, non-citrate-exclusive substrate range was predicted for this protein [15]. This function led to the characteristic naming of TctABC and its homologues as tricarboxylate transporters.

To date, only a small number of TTT SBPs have been biochemically characterized alongside TctC. Crystal structures obtained from the Bug family of TTT SBPs present in *B. pertussis* initially revealed that transporters within this family may have a substrate range that is more diverse than originally proposed, with some of these Bug SBPs clearly possessing the ability to bind dicarboxylic acids such as aspartate, glutamate and nicotinate [11,16,17]. The affinity of certain TTT SBPs for dicarboxylic acids has more recently been reinforced through the identification and characterization of the SBPs AdpC [5] and MatC [18] in *R. palustris*, which bind mid- to long- chain length dicarboxylic acids. Interestingly, the expression of both SBPs in their respective systems seems to be regulated by low substrate concentrations, suggesting that a regulatory system has been evolved which enables the organism to adapt to different substrate availability in its environment.

1.3. The TRAP Transporter Family

The discovery of TRAP transporters occurred in the 1990's, when findings on the first ever fully described TRAP system, DctPQM, from *R. capsulatus* (DctP, DctQ and DctM being the periplasmic, small transmembrane and large transmembrane domains, respectively) were published [4]. Purification and characterization of DctP prior to this study had already led to the discovery that this system was involved in C4-dicarboxylate uptake [19,20], however it was only after sequencing of the genes neighbouring *DctP* (*DctQ* and *DctM*) that distinguishment was made between this transporter and ABC transporters [4]. The transmembrane subunit-encoding genes *DctQ* and *DctM* showed very little sequence similarity to the genes that are ordinarily found to flank the SBP component in ABC systems, and clear insensitivity of DctPQM to orthovanadate, a known ABC transporter inhibitor, supported a distinction from the ABC transporter superfamily [4]. Moreover, uncoupler

titration experiments further demonstrated that the level of succinate transport by DctPQM is indeed dependent on membrane potential. The supplementation of increasing concentrations of uncoupler compounds like carbonyl cyanide m-chlorophenyl hydrazone (CCCP), as well as others that likewise disrupt the proton gradient of the cytoplasmic membrane, greatly reduced the rate of succinate transport by DctPQM [4]. Furthermore, the subsequent addition of ATP at severely low/zero membrane potential was not able to rescue the rate of succinate transport [4], thereby reinforcing the conclusion that this system is indeed a secondary ATP-independent transporter.

Subsequent studies on TRAP systems have identified a multitude of different TRAP transporters that exist across bacteria and archaea [21–25]. As is the case with TTT transporters, most research has focussed on the extracytoplasmic components of these systems and has thus led to the discovery of three distinct types of TRAP transporter based principally, but not exclusively, on their SBPs [7]. These subdivisions include the DctP-like 'classical' group of TRAP transporter (1.3.1), as well as the TAXI-TRAP group (1.3.2) and the tetratricopeptide motif-protein (TPR) associated transporter (TPAT) group (1.3.3).

1.3.1. The Classical TRAP Group

Since the discovery of DctPQM, many TRAP transporter SBPs have been crystallized and/or biochemically characterized; with the classical TRAP group of SBPs representing the largest subdivision of TRAP SBPs that have thus far been researched. Genome sequence analysis that occurred after the characterization of DctPQM identified several *dctP* gene homologues that exist within a multitude of prokaryotes but are absent from eukaryotes [22]. This led to further research on specific DctP homologues and consequentially, by 2010, seven different, but structurally very similar, DctP-like TRAP SBPs were crystallized from numerous organisms (Table. 1) [25].

Table 1. Crystallized classical TRAP SBPs from various organisms. Adapted from Fischer *et al.* [25], this table represents all known structures of DctP-like SBPs up to the year 2010. Nearly all proteins were co-crystallized with their respective substrates, thus demonstrating the wide range of carboxylic acids that can be transported by this class of TRAP transporter.

SBP	Source organism	Protein data bank (PDB) ID	Resolution (Å)	Conformation	Ligand
SiaP	*Haemophilus influenzae*	2CEX	2.20	Closed	Neu5Ac2en
		3B50	1.40	Closed	Sialic acid
		2CEY	1.70	Open	-
TakP	*Rhodobacter sphaeroides*	2HZL	1.40	Closed	Sodium pyruvate
		2HZK	1.70	Open	Glycerol
DctP7	*Bordetella pertussis*	2PFY	1.95	Closed	Pyroglutamate
DctP6	*Bordetella pertussis*	2PFZ	1.80	Closed	Pyroglutamate
TeaA	*Halomonas elongata*	2VPO	1.80	Closed	Hydroxyectoine
		2VPN	1.55	Closed	Ectoine
UehA	*Silicibacter pomeroyi*	3FXB	2.90	Closed	Ectoine
TM0322	*Thermotoga maritima*	2HPG	1.90	Closed	Unidentified
LakP	*Thermus thermophilus*	2ZZV	1.40	Closed	Calcium lactate
		2ZZW	1.95	Closed	Zinc lactate
		2ZZX	1.75	Closed	Lactic acid

These defined members of the classical TRAP system are prominent within human pathogens and, fittingly, the best studied TRAP system to date, SiaPQM from *H. influenzae*, was found to be essential for the uptake of sialic acid; a key component of lipopolysaccharide (LPS) which contributes to bacterial resistance against human serum [26–28]. SiaPQM also remains to be the only TRAP system to ever be fully reconstituted and have its complete transport mechanism characterized. In their study, Mulligan *et al.* found that sodium-coupled sialic acid transport by SiaQM is exclusively dependent on its specific SBP, SiaP, which not only offers a means for high affinity uptake of substrate, but also provides transport unidirectionality to the system [24]. That said, it was found that sodium-coupled sialic acid export is possible for this system, however it is only induced when extracellular unsaturated SiaP concentrations are in excess [24]. Homologous systems to SiaPQM were subsequently found in various human pathogens, including *V. cholerae* and *V. vulnificus* [29], as well as numerous other pathogens [30,31].

As well as being the first TRAP system to have its method of transport fully defined, SiaPQM was also the first of now numerous secondary ion-dependent transporters to have its SBP component crystallized. Despite being dissimilar at sequence level to SBPs from the ABC transporter superfamily, the overall topology of SiaP was found to be analogous to ABC SBPs [32], which appears to reinforce the implication that these families have an evolutionary link. An insight into the crystal structures of 7 different DctP-like SBPs showed that there were

some key similarities between members within this subdivision of TRAP SBPs [25]; including conservation of ligand positioning within the binding pocket (although variability in hydrophobic interactions and hydrogen bonds makes predicting substrate ranges for uncharacterized DctP-like SBPs problematic) and a long α-helical hinge that kinks by ~ 30 Å upon ligand binding [25,32]. Most significantly, however, was the discovery of a conserved arginine residue (localized in domain 2) amongst these 7 SBPs that was first identified in SiaP and found to be involved in the formation of a salt bridge with the carboxylate group of sialic acid [32]. Clearly, this arginine is a critical component for ligand binding in this group of SBPs, acting as a high affinity selectivity filter for the transport of carboxylic acids [33] and therefore a defining feature for this group.

1.3.2. The TAXI-TRAP Group

The TAXI-TRAP subdivision of transporters describes a group of TRAP systems that, unlike classical TRAP transporters, have SBPs that show very little sequence homology to DctP and are the only form of TRAP transporter that is seen within archaea [1]. The name TAXI originates from the first example of a TAXI protein to be recognised in literature, when Mayfield *et al.* depicted the cloning and expression of a 31 kDa cell surface 'immunogenic' protein from *B. abortus* [34], whose function has yet to be defined. As well as having a family of SBPs that are distinct from DctP, TAXI-TRAP systems were also found to have another significant difference compared to classical TRAP transporters; a single membrane domain that is derived from the fusion of the two integral membrane components, often due to the addition of an extra transmembrane subunit (see Fig. 2) [7,22].

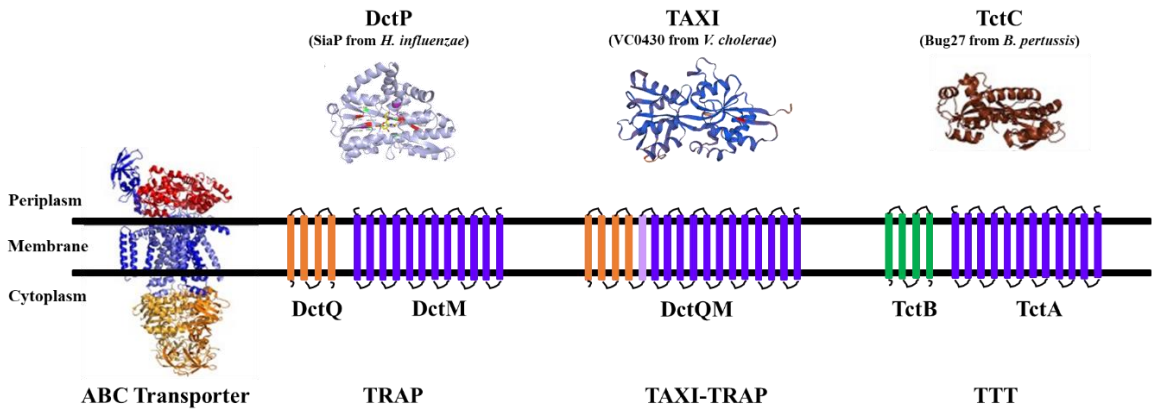

Figure 2. Topologies and structural examples of SBP-dependent transporter systems. The example ABC transporter is the maltose transporter MalEFGK2 from *E. coli*; formed of an SBP component (red), two transmembrane domains (blue) and two nucleotide-binding domains (orange). In the SBP-dependent transporters, the orange and green subunits represent the 4-transmembrane helical domains for both TRAP and TTT systems, respectively. The blue subunits make up the 12-transmembrane domains for all systems, whilst an additional subunit (purple) in TAXI-TRAP systems acts to fuse both transmembrane domains together. Figure adapted from Rosa *et al.* [7].

Despite being discovered over 20 years ago, the TAXI-TRAP group of transporters remains one of the most poorly described members of the secondary SBP-dependent transporter family. A full biochemical characterization of a TAXI-TRAP system or SBP is still absent from literature, however, a small number of studies on certain TAXI SBPs has provided some clues as to what the function of these proteins may be within bacteria and archaea. A paper by Rabus *et al.* in the late 1990's provided the first hint of a potential substrate range of these proteins; TAXI SBPs from *A. fuldigus* and *H. influenzae* shared significant sequence similarity to well-characterized glutamate- and glutamine- transporters from the ABC transporter family in *E. coli* [21]. This suggested substrate range was later reinforced when the first and thus far only crystal structure for a TAXI SBP was published by Takahashi *et al.* in their study of TtGluBP; a TAXI SBP from *T. thermophilus* HB8 that was found co-crystallized with either L-glutamate or L-glutamine in its binding site [35]. Nevertheless, almost half a decade later, Bakermans *et al.* reported their findings of a gene knockout study in which a significant decrease in growth of *P. arcticus* on acetate-, butyrate- and fumarate- enriched media was observed when *DctT,* the gene encoding the SBP component of a TAXI-TRAP system, was removed from the genome [36]. This was first was piece of evidence to suggest that TAXI-TRAP systems may have a wider substrate range than originally thought, however there has since been some more data published that upholds this claim.

In their insightful review, Mulligan *et al.* provided some support of a wide substrate range for TAXI-TRAP transporters by analysing the genome context of several TAXI-TRAP gene clusters from different organisms, whereby neighbouring genes encoding enzymes involved in the metabolic pathways of potential substrates were used as indicators of the system's function [1]. Intriguingly, and most recently, a TAXI-TRAP system within *Azoarcus sp.* CIB, a denitrifying bacterium involved in the degradation of aromatic compounds [37], has been shown to uptake ortho-phthalic acid under aerobic conditions and use it a sole carbon source for growth [38]. This not only has substantial implications on our understanding of the function of TAXI-TRAP transporters, but also demonstrates their potential to be used in the development of bioplastics and in the plastic recycling industry.

1.3.3. The TPAT Group

In their study of the syphilis-causing pathogen *T. pallidum*, Deka *et al.* identified a third type of TRAP transporter that is distinct from both the classical TRAP and TAXI-TRAP systems [39]. As an obligate pathogen, *T. pallidum* has a heavy dependence on transport systems to scavenge the biomolecules needed for basic growth and survival from its human host. This considered, Deka *et al.* proceeded to analyse the genomic context of a TRAP transporter identified within the organism, as well as provide an overview of the crystal structures of

some of its constituents. Interestingly, it was found that the typical PQM components of the TRAP transporter belong in the same operon as an additional gene, *TatT*, which encodes a TPR protein that usually participates in protein-protein interactions [39,40]. Through crystallography, this TPR protein was shown to associate with the SBP component of the transporter ($TatP_T$) in a conformation which sees the C-terminal side of the pore in TatT align with the substrate-binding site of $TatP_T$ (see Fig. 3B), creating a complex which is strongly indicative of some form of substrate exchange between the two proteins [41]. Additionally, the crystal structure of $TatP_T$ revealed that its binding site is hydrophobic; a feature that is not seen in other TRAP SBPs, which predominantly bind negatively charged ligands, and is therefore suggestive of a drastically different substrate range that may involve the binding of lipids [39,41]. The distinct interaction of $TatP_T$ and TatT in the system has been predicted through a hypothetical transport model (Fig. 3) [41], however biochemical characterization and/or reconstitution of one of these systems would confirm the transport mechanism of this subdivision of TRAP transporters.

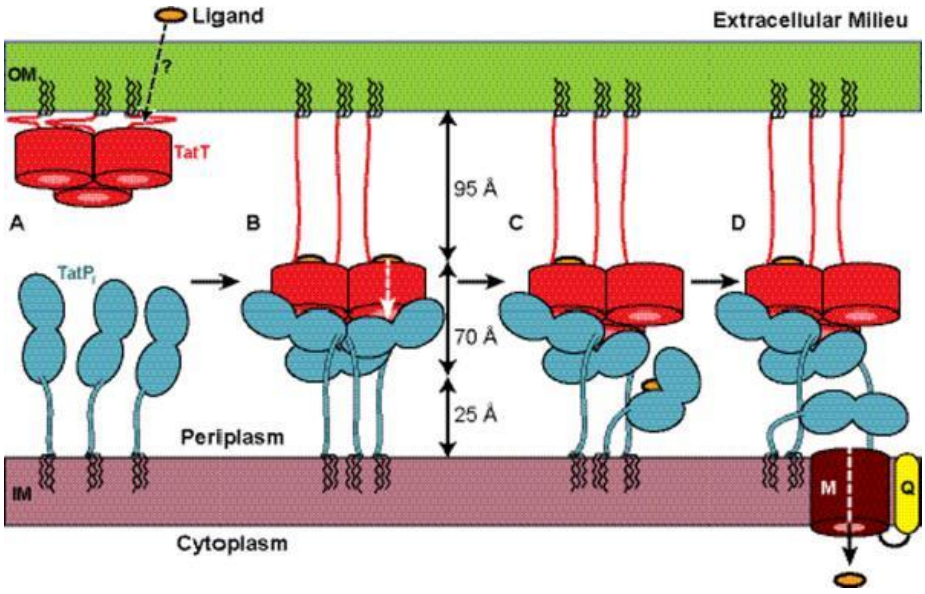

Figure 3. Hypothetical topology and transport model for the TPAT group of TRAP transporters. This model uses the TPAT system identified in *T. pallidum* as an example. (**A**) The outer membrane (OM) domain of the transporter (TatT, red) binds to its ligand and (**B**) escorts it across the periplasm where it is subsequently presented to the SBP domain ($TatP_T$, blue). (**C**) The SBP binds tightly to its ligand and dissociates from the OM domain before (**D**) delivering it to the transmembrane symporter domains for transport across the inner membrane (IM). An electrochemical ion gradient fuels the final step in this transport mechanism but, for simplicity, this was excluded from the illustration. Figure is taken from [41].

1.4. Project Objectives

To date, there is very little information available in literature on the TAXI-TRAP family of secondary transporters, and a full biochemical characterization of a TAXI-TRAP SBP has not previously been attempted. Hence, the aim of this project is to elucidate the structure and function of VC0430, a TAXI-TRAP SBP from *V. cholerae*, using both computational and biochemical techniques to provide novel insight on the TAXI-TRAP family. We also endeavour to use our findings to make hypotheses about the role of VC0430 and its substrates in the survival and pathogenicity of *V. cholerae*, with VC0430 predicted to provide a potential target for the development of antibiotic-alternative drugs to combat disease.

To achieve our goals, we performed a variety of experiments. These are summarized as follows:

- Using various computational techniques, including genome analysis and homology modelling, to predict structural and functional properties of VC0430.
- Optimising expression and purification protocols to generate VC0430 samples for future experiments/assays.
- Size-exclusion chromatography to establish the physical characteristics of VC0430.
- Binding assays (including thermal shift assays, fluorescence spectroscopy and microscale thermophoresis) to determine the substrate range of VC0430.

CHAPTER 2: MATERIALS & METHODS

2.1. Strains, Plasmids, Media & Buffers

2.1.1. *E. coli* strains

Table 2. List of all *E. coli* strains used for this project.

Strains of *E. coli*	Source	Genotype
BL21 (DE3)	Robinson Lab, University of Kent	F–ompT hsdSB (rB–, mB–) gal dcm (DE3)
TOP 10	Invitrogen	F– mcrA Δ(mrr-hsdRMS-mcrBC) ϕ80lacZΔM15 ΔlacX74 recA1 araD139 Δ(ara-leu)7697 galU galK λ– rpsL(StrR) endA1 nupG
NEBTurbo	NEB	glnV44 thi-1 Δ(lac-proAB) galE15 galK16 R(zgb210::Tn10)TetS endA1fhuA2 Δ(mcrB-hsdSM)5, (rK – mK –) F'[traD36 proAB+ lacIq lacZΔM15]

2.1.2. Plasmids

Table 3. List of plasmids used in this project. Note that pRY15 is the same gene as VC0430, just embedded within a different vector; pET206.

Plasmid	Source organism	Characteristics
pEThisVC0430WT	*Vibrio cholerae*	Kan^r
pET206pRY15WT	*Vibrio cholerae*	Amp^r

2.1.3. Media

Table 4. Media used for the growth and expression of *E. coli* transformants. All media listed here was used in procedures such as transformations, growth of cell cultures and expression of TRAP SBPs.

Media	Composition
Lysogeny broth (LB)	For 1L: 10 g NaCl, 10 g tryptone, 5 g yeast extract- added to MilliQ water and sterilised by autoclaving
LB Agar	For 1L: 10 g NaCl, 10 g tryptone, 5 g yeast extract, 15 g agar- added to MilliQ water and sterilised by autoclaving
Super optimal broth with catabolite repression (SOC)	0.5 % Yeast extract, 2 % tryptone, 10 mM NaCl, 2.5 mM KCl, 10 mM MgCl2, 10 mM MgSO4, adjust to pH 7.5 using NaOH. Autoclave and add filter sterilised 1 M glucose

2.1.4. Solutions & Buffers

2.1.4.1. Protein Extraction & Purification Buffers

Table 5. Buffers used for protein extraction and purification. These buffers were used in standard nickel affinity chromatography to purify TRAP SBPs in the form by which they are expressed.

Buffer	Composition
Lysis buffer	50 mM Tris pH 8, 200 mM NaCl, 5% glycerol- made up to volume with MilliQ
Wash buffer	20 mM imidazole- made up to volume with lysis buffer
Elution buffer	300 mM imidazole- made up to volume with lysis buffer

Table 6. TRAP SBP renaturation using a GHCl gradient. To denature and refold TRAP SBPs, decreasing concentrations of GHCl were used during the wash step in nickel affinity chromatography. Volumes displayed here were made up by adding MilliQ and were suitable for the renaturation of protein from 25 mL of clarified lysate. Larger/smaller volumes of clarified lysate required renaturation buffer volumes to be scaled accordingly.

Standard composition	Concentration of GHCl (M)	Total buffer volume (mL)
50 mM KPi 200 mM NaCl 20% Glycerol 20 mM Imidazole	2.0	15
	1.5	2
	1.0	2
	0.5	2
	0	4

2.1.4.2. General Solutions & Buffers

Table 7. Summary of the main solutions and buffers used in this report. Above are the buffers/solutions used for the collection of all the main data in this project. Buffers/solutions used during optimisation are excluded from this table.

Solutions/Buffers		Composition	
SDS GEL COMPONENTS	SDS page gel	Resolving: 6.9 mL Bisacrylamide, 2.6 mL 1.875 M Tris pH 8.8, 130 µL, 10% SDS, 3.77 mL dH2O, 130 µL 10% APS and 13 µL Tetramethylethylenediamine (TEMED) Stacking: 1.69 mL Bisacrylamide, 1.625 mL 1 M Tris pH 6.8, 130 µL 10% SDS, 9.56 mL dH2O, 130 µL 10% APS and 13 µL TEMED	
	10X SDS running buffer	30 g Tris, 150 g glycine, 10 g SDS- made up to 1 L with MilliQ	
	4X SDS sample buffer	12 g glycerol, 10 mL 10 % SDS, 1 mL 1 M Tris pH 7.2, 0.06g Bromophenol Blue and 3 mL MilliQ	
	Coomassie brilliant blue dye	50 % Methanol, 50 % acetic acid, 0.2% Coomassie Blue	
	Coomassie destain	Methanol 20%, acetic acid 10%- made up to 1 L with 700 mL MilliQ	
ASSAY BUFFERS	Thermal shift assay buffer	50 mM KPi pH 7.8, 20 mM NaCl- made up to volume with MilliQ	
	Tryptophan fluorescence assay buffer	50 mM Tris pH 7.5- made up to volume with MilliQ	
	Microscale thermophoresis assay buffers	20 mM NaCl, 50 mM KPi pH 7.8, 0.05% Tween- made up to volume with MilliQ	1X PBS-T Buffer, supplied by NanoTemper
SEC BUFFER	SEC buffer	50 mM Tris pH 7.5- made up to volume with MilliQ (degassed)	
ANTIBIOTICS	Kanamycin (kan)	In all media it was used in, the working concentration of kan was 50 µg/mL	
	Ampicillin (amp)	In all media it was used in, the working concentration of amp was 100 µg/mL	

2.2. Molecular Biology Techniques

2.2.1. DNA Miniprep

For all minipreps, the QIAprep kit (Qiagen) was used to purify plasmid DNA. To begin with, 5 mL of antibiotic selective LB (either LBkan or LBamp) was inoculated with cells, from glycerol stocks stored at -80 °C, containing the plasmid to be purified. The culture was left to grow overnight in a shaking incubator at 190 rpm, 37 °C. The next day, cells were lysed, and plasmid DNA was purified as per the instructions given in the QIAprep kit. Purified plasmid DNA concentration was measured using a nanodrop and was then stored at -20 °C for future use.

2.2.2. Transformations

Under sterile conditions, *E. coli* cells from the desired strain (from glycerol stocks) were used to inoculate 5 mL of LB before being left overnight to incubate at 37 °C, at a 190 rpm shake (standard conditions). The following day, 500 µL of the culture was refreshed in 4.5 mL of LB and left to incubate for an hour under standard conditions. Thereafter, 833 µL of culture was distributed amongst sterile 1.5 mL Eppendorf tubes and cells were harvested by microcentrifugation for 1 minute at 13000 xg. The resulting pellets were then each resuspended in 50 µL ice-cold 100 mM $CaCl_2$, creating multiple 50 µL shots of chemically competent cell suspensions.

2.2.2.1. Transformation by Heat-Shock

100 ng of plasmid DNA was mixed into a single 50 µL shot of competent cells and left on ice for 30 minutes. After this incubation, the mixture was immediately heated for exactly 1.5 minutes at 42 °C in a dry heating block to allow the plasmid to enter the cells. Following that, 200 µL of SOC was added to the mixture and left to incubate under standard conditions. After 1 hour, 10 µL of the transformant mixture was added to a selective LB plate and left to incubate overnight at 37 °C. Colonies of transformed cells were observed and counted the next day.

2.2.2.2. Transformation by Freeze-Thaw

100 ng of plasmid DNA was mixed into a single 50 µL shot of competent cells before being left to snap-freeze on dry-ice-ethanol for 1.5 minutes. After this, the mixture was immediately thawed for exactly 2 minutes at 37 °C in a dry heating block to allow the plasmid to enter the cells. Following that, 200 µL of SOC was added to the mixture and left to incubate under standard conditions. After 1 hour, 10 µL of the transformant mixture was added to a selective LB plate and left to incubate overnight at 37 °C. Colonies of transformed cells were observed and counted the next day.

2.3. Expression of TRAP SBPs

Note: see Table. 7 for antibiotic-specific concentrations that were used during all steps of expression where the presence of antibiotic was required

After successfully transforming competent *E. coli* cells with the desired plasmid, one colony from the selective LB agar plate was used to inoculate 5 mL of LB + antibiotic (LB_{ab}). This culture was left to grow under standard conditions for at least 4 hours before being refreshed into 50 mL LB_{ab} for growth overnight. The following day, 20 mL of overnight culture was used to inoculate 1 L of LB_{ab} and growth under standard conditions was monitored by spectrophotometric absorbance at a 600 nm optical density (OD_{600}). Once OD_{600} had reached 0.6 – 0.8, the cultures were induced with 1 mM isopropylthio-β-galactoside (IPTG) and left to continue incubation overnight. Cells were harvested by centrifugation at 4000 xg, 4 °C, and resulting pellets were resuspended and homogenised in 50 mL lysis buffer (see Table. 5) per litre of culture. The cell suspension then underwent sonication for 10 minutes at 8 kHz (3 seconds on, 7 seconds off with a 2.5 minute rest period after the first 5 minutes of sonication) before the resultant lysate was clarified by centrifugation at 20,000 xg, 4 °C. The clarified lysate then proceeded to the purification step, which is described in the next section.

2.4. Purification of TRAP SBPs

2.4.1. Nickel Affinity Chromatography

Clarified lysate from the protein expression step was required to undergo further processing to isolate purified protein. To purify TRAP SBPs, immobilized metal affinity chromatography (IMAC) using Nickel-chelating nitrilotriacetic acid (Ni-NTA) resin (Qiagen) was performed at room temperature.

Firstly, a 25 mL purification column suspended on a clamp was prepped with 1 mL of Ni-NTA resin (0.5 mL column volume, CV) and left to rest for ~2 minutes before being washed through with 5 CV MilliQ and then equilibrated with 5 CV of lysis buffer. 25 mL of clarified lysate was subsequently added to the sealed column and left to sit for 10 minutes to allow polyhistidine (his)-tagged protein to bind with high affinity to the resin. After the incubation period, the column was unsealed and the flow through of clarified lysate was collected. Next, 20 CV of wash buffer was added to the column and allowed to fully flow through (washing step). Protein was then eluted in 5 fractions using elution buffer containing 300 mM imidazole, which dislodges protein from the resin. The first fraction was eluted using 0.5 CV of elution buffer, whilst all subsequent fractions were eluted after the addition of 2 CV elution buffer. Fractions collected were spectrophotometrically measured for their absorbance at 280 nm

(A280) and using the Beer-Lambert law and predicted extinction coefficient (AAT Bioquest online tool), protein concentration was determined. 15 µL of all samples were also used for analysis by SDS-PAGE after the addition of 5 µL 4X SDS sample buffer.

Protein renaturation was performed in some cases where the SBP was suspected to be prebound to ligand after expression. SBPs that happen to be saturated during growth and expression are unfavourable for use in subsequent assays, so refolding of SBPs during IMAC eliminated this issue. TRAP SBPs were renatured during the 'washing step', whereby the single wash step described above was substituted by a gradient GHCl wash series (see Table. 6).

2.4.2. Size Exclusion Chromatography

Size exclusion chromatography (SEC) of TRAP SBPs that had previously undergone IMAC was performed using a 24 mL Superdex 200 Increase 10/300 GL column at a 0.5 mL min^{-1} flow rate in an AKTA purification system. After IMAC, elution fractions containing nickel affinity chromatography-purified protein were combined and underwent volume reduction to 1 mL; the resulting solution was then ultra-centrifugated at 60,000 rpm, 4 °C. The SEC column was washed with degassed MilliQ before being equilibrated with degassed SEC buffer (see table. 7). The supernatant of the ultra-centrifugated product was loaded into the column and fractions of SEC purified protein were collected. A basic breakdown of the overall purification steps for proteins used in assays is portrayed in Fig. 4.

To determine the molecular characteristics of the TRAP SBPs in question, such as molecular weight and Stoke's radius, a calibration curve was generated using the SEC standards ribonuclease A (13.7 kDa), carbonic anhydrase (29 kDa), ovalbumin (44 kDa) and ferritin (440 kDa). K_{av} (partition coefficient) was calculated from the equation: $K_{av} = (V_e - V_o)/(V_t - V_o)$, where V_e is the elution volume for a given protein, V_o is the column void volume and V_t is the total volume of the column.

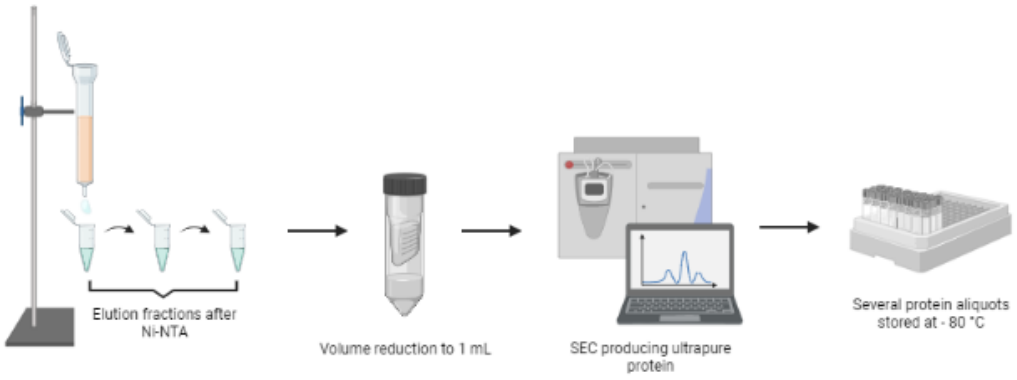

Figure 4. Significant steps for purification of TRAP SBPs from clarified lysate. Clarified lysate obtained from growth and expression first underwent nickel affinity chromatography, producing fractions of eluted protein. Purified protein was then combined, and the overall volume of the sample was reduced to 1 mL. Protein then

underwent further purification by SEC, producing a large concentration of ultrapure protein. Figure was created with BioRender.com.

2.5. Thermal Shift Assay

All thermal shift assays were completed in a QuantStudio 3 RT-PCR machine and experimental design (Fig. 5) was carried out on the accompanying QuantStudio Design & Analysis Software (Thermo Fisher). Substrates used for screening were made up prior to the assay at a stock concentration of either 60 mM or 30 mM in MilliQ and were carefully adjusted to a pH of between 7.0 – 7.5 using KOH. Triplicate 50 µL samples of 5 µM protein, 100 µM or 1 mM substrate and 3.5x SYPRO Orange Dye (Merck) made up in assay buffer (see Table. 7) were pipetted into low-profile PCR tube strips (Bio-Rad) and mixed using a desk-top microfuge for 30 seconds at ~ 2500 xg before each run. Post-run data was exported and plotted in Microsoft Excel.

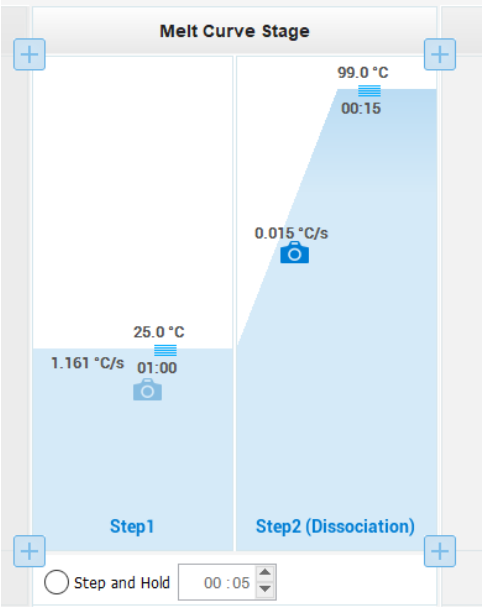

Figure 5. Experimental design of Thermal Shift Assays using QuantStudio Design & Anaysis Software. To begin with, thermocycler temperature was cooled to 25 °C at a rate of 1.161 °C s^{-1}. This temperature was then held for 1 minute, before gradually increasing at a rate of 0.015 °C s^{-1} with fluorescence readings being taken at every increment. Once a maximum temperature of 99 °C was reached, it was held for 15 seconds prior to the run ending. The reporter dye setting was set to 'ROX' and the passive reference set to 'none'.

2.6. Intrinsic Tryptophan Fluorescence

The intrinsic tryptophan fluorescence of VC0430 was measured using a Cary Eclipse fluorimeter (Agilent) in a quartz cuvette containing 2 mL assay buffer (Table. 7) and 0.5 µM protein. For titration data, increasing concentrations of substrate were added to the protein solution and the fluorescence change was measured. Excitation was always kept at 280 nm; for emission scans, emission data was collected over a range of 290 nm – 500 nm and for

titration data, the emission wavelength was fixed at 330 nm with fluorescence being captured every half second. Slit width was kept constant at 5 nm for both excitation and emission for all datasets collected. Experimental design was greatly influenced by the protocol published by Yammime *et al.* [43] and estimation of the dissociation constant (K_d) between VC0430 and any of its potential targets was determined using r^2-dependent curve fitting in excel.

2.7. Microscale Thermophoresis

Second Generation RED-tris-NTA dye (Monolith His-Tag Labelling Kit, NanoTemper) was used to label VC0430 prior to attempts at microscale thermophoresis (MST); this will be further discussed later in the 'Results' section. To determine the affinity of the dye to VC0430, the instructions for experimental setup provided by the kit manual were followed. Starting at a concentration of 2 µM, a 16-step serial dilution of VC0430 was performed- with the protein being diluted 1:2 with 1X PBS-T buffer at each step. RED-tris-NTA dye was then added to each of the protein samples in the dilution series at a final concentration of 25 nM. The protein-dye samples were incubated at room temperature for 30 minutes before being loaded into MST capillaries. Readings were taken at 40% LED power and 40% MST power using the Monolith NT.115 system provided by NanoTemper. Data analysis was performed using the accompanying NanoTemper analysis software.

2.8. Homology Modelling & Binding Site Mapping of VC0430

The predicted structure of VC0430 was generated by automated homology modelling using the SWISS-MODEL online tool. The model was formed based on a template provided by an unnamed immunogenic protein from *Ehrlichia chaffeensis*. For simplicity purposes, this template is referred to by its PDB ID (4DDD) throughout this report. The suitability of the template and the significance of its homology to VC0430 will be discussed in detail later on in the 'Results' chapter. Binding site mapping was performed with ChimeraX, using TtGluBP from *T. thermophilus* as a comparative model.

CHAPTER 3: RESULTS

3.1. Computational Analysis of VC0430

Past research on transporters in *V. cholerae* has identified systems/constituents that contribute to the transport of carboxylic acids across the membrane [44,45]. Recently, VcSiaP, a SBP from the sole sialic acid transport system in *V. cholerae*, has been explored as a potential drug target [6]. Initial screening of artificial peptides for this TRAP SBP, using crystallography and digital fluorescence imaging of binding events, has shown that it is possible for synthetic substrates to bind VcSiaP at micromolar affinity, thus providing a starting point for the development of VcSiaP inhibitors [6] and opening the possibility for inhibitors of other TRAP SBPs to be designed.

VC0430 has previously been identified as a TAXI-TRAP SBP from *V. cholerae* [22], and our interest in characterizing this SBP descends from its potential to be a drug target, much like VcSiaP. It is also a constituent of a TAXI-TRAP system; a transporter family that is present within several other pathogens, including *P. aeruginosa* and *R. prowazekii*, and has not been biochemically characterized before. Computational analysis was performed to provide a starting point for the biochemical characterization of VC0430. By ascertaining its structure, along with examining the SBP in the context of its operon, we aimed to make predictions about its function. This would provide the basis of subsequent *in vitro* attempts at distinguishing the substrate range of VC0430.

3.1.1. Genome Context of VC0430

VC0430 from *V. cholerae* is composed of 328 amino acid residues, however the fully mature protein that exists after signal peptide cleavage is likely to consist of 297 residues. The *vc0430* gene is embedded within a standard operon for TAXI-TRAP transporters, whereby it is followed by a fused gene that encodes the membrane components of the system (Fig. 6). The purpose of examining the operon that this system belongs to was to find any clues which may give some indication of the protein's function. Initial analysis of the operon identified a gene encoding malate dehydrogenase (MDH) upstream of the transporter-encoding genes, leading to the prediction that VC0430 may bind malate and potentially some other C4-dicarboxylates/carboxylic acids.

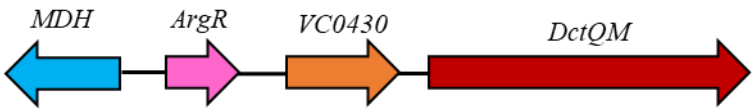

Figure 6. Genetic neighbourhood of *VC0430 in V. cholerae*. *VC0430* directly follows a fused membrane component (homologous to *DctQM* from *R. capsulatus*) which is a characteristic feature of TAXI-TRAP systems. Further upstream of the TAXI-TRAP genes lies an arginine pathway regulatory protein (ArgR) gene, which is closely followed by a gene encoding MDH.

3.1.2. Multiple Sequence Alignment of TAXI-TRAP SBPs

A multiple sequence alignment of TAXI-TRAP SBPs was performed using the sequences of some of the SBPs which were originally identified by Kelly *et al.* [22] as well as others that were found through searches of databases such as MicrobesOnline and Pfam (Table. 10). Analysis of the multiple sequence alignment was facilitated by WEBLOGO (Fig. 7), with the hope that an obvious conserved residue(s) would be found which might give an indication of the substrate range of TAXI-TRAP transporters- as is the case with the conserved arginine in the Classical TRAP group. Unfortunately, no such residue could be identified, however this may suggest that the TAXI-TRAP group has a very wide substrate range which is most likely not restricted to just carboxylic acids.

Despite the absence of an obvious carboxyl group selector, it is clear that there are a few other very well conserved residues amongst the eleven TAXI-TRAP SBPs we assessed. The most apparent residue that is highly conserved is glycine, whilst proline, histidine and glutamate also seem to be well conserved throughout the genomes. These residues, along with any others that may be of interest, present attractive targets for any future work involving site-directed mutagenesis (SDM) and could help to provide evidence of a general function for TAXI-TRAP SBPs, as was the case for the Classical TRAP group.

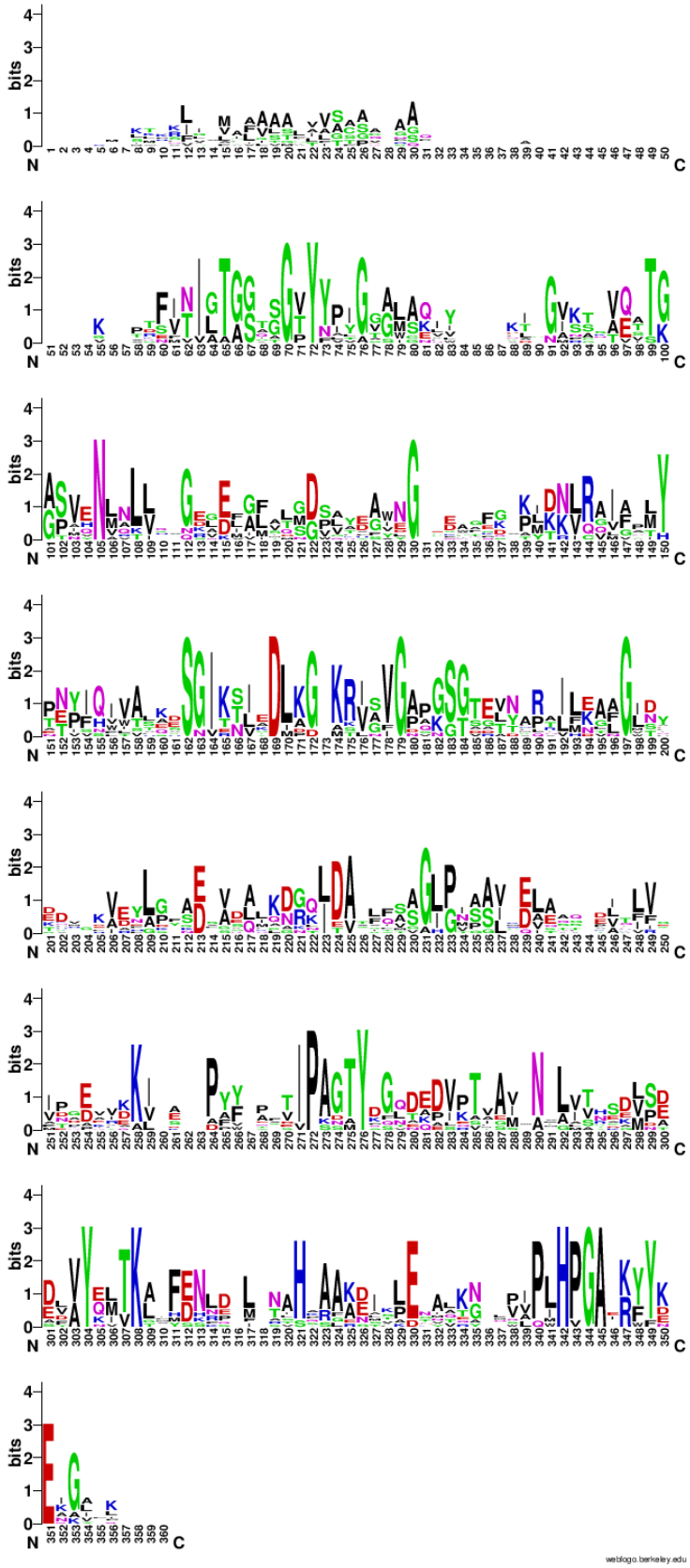

Figure 7. WEBLOGO summary of the TAXI-TRAP SBP multiple sequence alignment. The alignment features sequences from 11 different SBPs (Table. 10). No standout residues that may give a hint towards the general function of TAXI-TRAP transporters could be identified. This data instead seems to be indicative of a substrate range that is highly variable amongst different proteins in this group.

Table 8. SBPs included within the multiple sequence alignment of TAXI-SBPs. TAXI-SBPs were identified in a range of organisms and their sequences were aligned (see Fig. 7 above).
* VC0430, the subject of this project
** GenBank number

Organism	Accession number
Psychrobacter ariticus	WP_011280027
Pseudomonas aeruginosa	WP_003114147.1
Vibrio cholerae	WP_001883255.1 *
Alkalihalobacillus halodurans	WP_010896778.1
Rhodopseudomonas palustris	WP_011474804.1
Candidatus Desulforudis audaxviator MP104C	ACA59767.1 **
Marinobacter algicola	WP_007154430.1
Pseudomonas stutzeri	WP_102839042.1
Archaeoglobus fulgidus	WP_010878139.1
Acinetobacter baumannii	WP_004785015.1
Cloacibacillus evryensis	WP_034442225.1

3.1.3. Homology Modelling and Binding Site Mapping of VC0430

Homology modelling using the SWISS-MODEL structure estimating software was used to generate a predicted model of VC0430 (see Fig. 8 and Fig. 9A), with the structure of 4DDD from *E. chaffeensis* used as a template. The Global Model Quality Estimate (GMQE) score was 0.77, thus indicating high overall model quality based on properties such as sequence identity (40.67%) and similarity, as well as agreement between the estimated secondary structures of both VC0430 and 4DDD [46]. Strong homology model quality for VC0430 was further supported by a QMEANDisCo Global score of 0.79 ± 0.05 which, like the GMQE score, is reassuringly high (scores for GMQE and QMEANDisCo Global are measured between 0 and 1, with larger numbers signifying higher model quality). The significance of QMEANDisCo scores on homology modelling is explained in detail by Studer *et al.* [47]. However, in short, it is a scoring function that qualitatively assesses estimates of interactions between residues in the model by considering residue-to-residue distances and distance constraints seen in homologous structures [47].

After the model for VC0430 was generated, initial examination of the structure identified two pairs of cysteines on opposite sides to each other (~ 34 Å apart) in the overall quaternary composition of the protein. This cysteine pair arrangement has not previously been recognised in literature based on other TRAP SBPs, and its involvement in protein stability and substrate-binding was something we thought could be explored. Additionally, the unpublished structure of 4DDD shows significant electron density for a disulfide bridge between its cysteine pairs, thereby suggesting that in VC0430 there is a reasonable chance that the cysteines in each pair may also form disulfide bonds with each other. Clearly, these two cysteine pairs provided attractive targets for future *in vitro* experiments with VC0430 (see

Results, 3.3.4.) but, interestingly, no significant conservation of these residues was highlighted by the multiple sequence alignment of TAXI SBPs described above (Fig. 7).

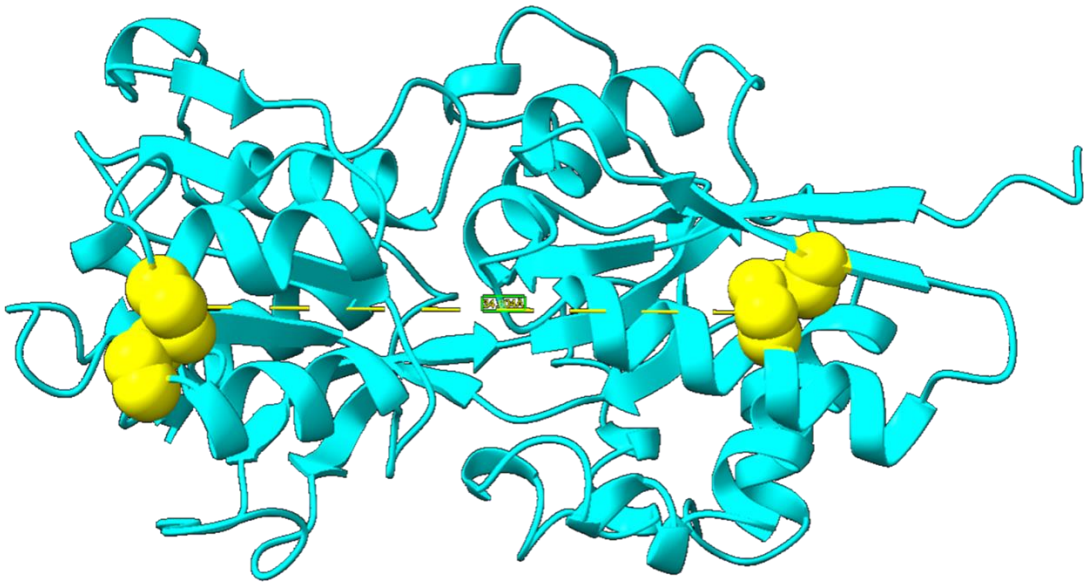

Figure 8. Structure of the VC0430 homology model with emphasis on the two opposite cysteine pairs. Cysteines (yellow) are arranged in pairs on opposite lobes of the VC0430 model and are ~ 34 Å apart. This arrangement was predicted to have some role in the overall stability and binding activity of the protein. The template structure used in homology modelling also seems to indicate the presence of disulfide bonds between the cysteines in each pair.

We next aimed to map the binding site of the VC0430 model against that of TtGluBP from *T. thermophilus*; a glutamate/glutamine binding protein which represents the only crystallized TAXI-SBP structure present in literature [35]. In their study of this protein, Takahashi *et al.* identified eleven residues in the binding site of TtGluBP which play a significant role in its binding mechanism through direct contacts with the substrate itself. Through a multiple sequence alignment between the VC0430 and TtGluBP, eight out of eleven of these residues were found to be conserved within VC0430 (Table. 11). Upon superimposing the structures of VC0430 and TtGluBP, which already bare a very strong overall conformational similarity, it could be seen that these conserved residues take up a similar arrangement in the binding sites of both proteins (see Fig. 9). This was the first major indicator that VC0430 may share a similar substrate range to TtGluBP, warranting further evaluation through *in vitro* experimentation.

Table 9. Key binding site residues in TtGluBP that are conserved within VC0430.
* Conserved residues
x Non-conserved residues

TtGluBP	Ser27	Val31	Tyr32	Phe33	Ser60	Gln78	Glu111	Gly142	Thr143	Tyr186	Thr187
VC0430	Ser40	Val44	Tyr45	Tyr46	Ser75	Gln93	Glu125	Gly156	Asp157	Tyr200	Met200
	*	*	*	x	*	*	*	*	x	*	x

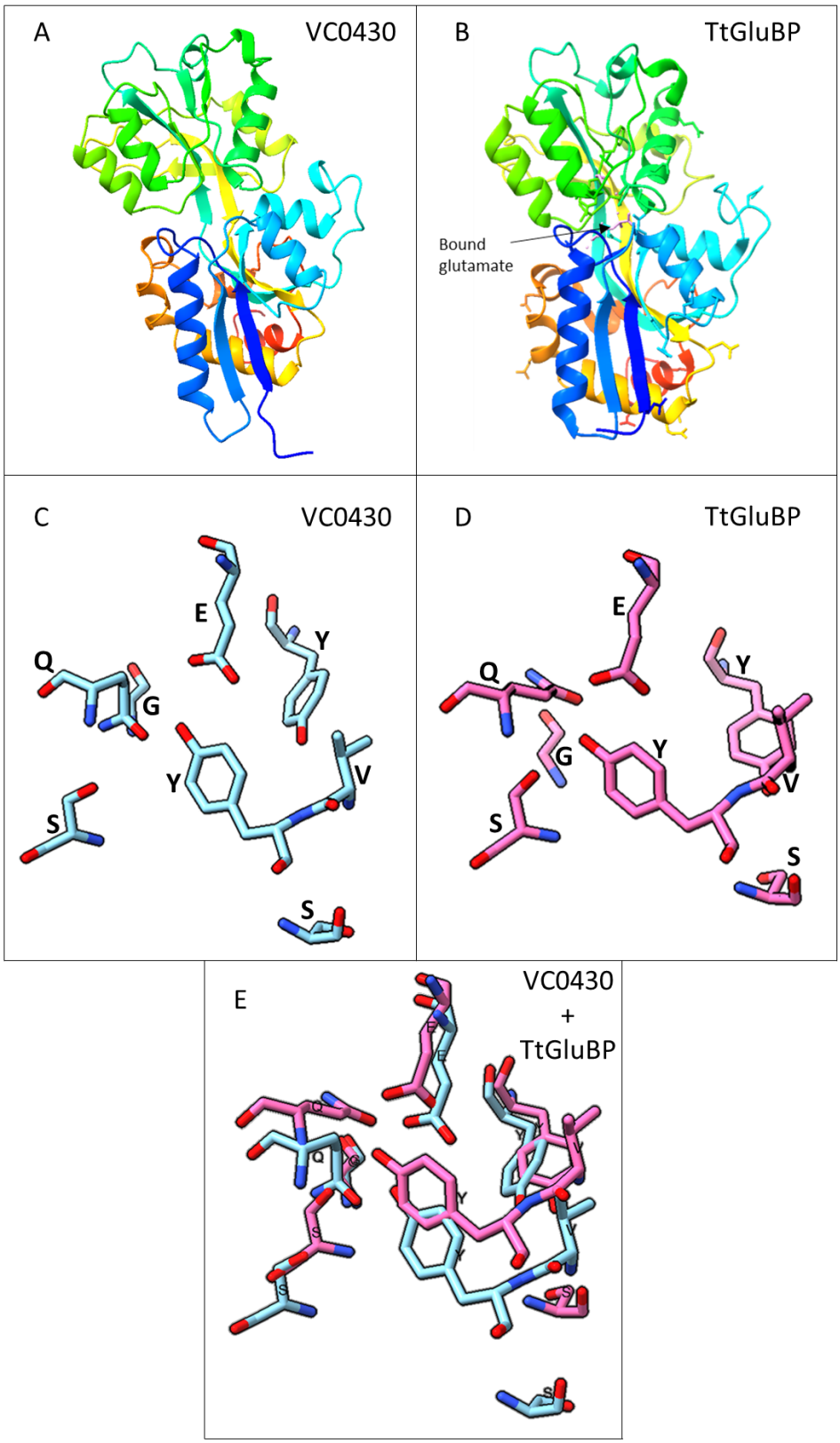

Figure 9. Structural comparison of VC0430 and TtGluBP. Panels A and B show the overall topologies of VC0430 and TtGluBP, respectively. For both proteins, domain 1 is represented in lime green and domain 2 is represented in dark blue, light blue and orange. The interdomain strands are shown in yellow and pale green. The crystal structure of TtGluBP was co-crystallized with L-glutamate, as indicated by the arrow. Panels C (VC0430) and D (TtGluBP) highlight the conserved binding site residues, labelled by their corresponding letters, and their conformations in both protein structures. Panel E displays the superimposition of the conserved residues shown in panels C and D.

3.2. Expression and Purification of TRAP SBPs

3.2.1. Overexpression and IMAC Purification of VC0430

Production of VC0430 was performed using two different pET expression vectors in order to assess the effect of His-tag positioning on *E. coli* (BL21 DE3) protein expression levels. One of the plasmids was employed to tag the protein at its N-terminus using a FLAG-His10-TEV tag (Fig. 10A); a 10X-His-tag linked with a relatively large polypeptide tag (FLAG-tag), consisting of a DYKDDDDK sequence motif (D= aspartic acid, Y= tyrosine, and K= lysine) [48,49], preceded by a tobacco etch virus (TEV) protease cleavage site. The other plasmid, pET-20b (also referred to in this report as pRY15), was used to express C-terminal 6X-His-tagged VC0430.

Both FLAG-His10-TEV- and C-terminal 6X-His- tagged VC0430 were overexpressed and purified before use in any following assay. Cells were grown in LB under standard conditions (as described in Materials & Methods, 2.2.2.) until they reached OD_{600}, at which point 1 mM IPTG was found to produce ample expression of VC0430. After harvesting and lysing cells, nickel-affinity chromatography was performed; enabling us to obtain pure VC0430 elutions, as demonstrated by the results of SDS-PAGE, with few contaminants (Fig. 10). Bands for VC0430 appear to be around the 30-35 kDa mark, and this was the size that was expected based on the online AAT Bioquest molecular weight predictor tool which gave an estimated value of 35 kDa. Our SDS-PAGE results also show that VC0430 tagged at the N-terminus by FLAG-His10-TEV (Fig. 10A) appears to express better than C-terminal 6X-His-tagged VC0430 (Fig. 10B), hence this plasmid was used for all proceeding attempts at protein expression. This means that FLAG-His10-TEV tagged VC0430 is what was used to generate all subsequent data in this report.

After initial thermal shift assays, when it was suspected that VC0430 may have been purified in its saturated form, denaturation of the protein was performed in an attempt to dislodge the substrate from the binding pocket. This was achieved through a series of wash steps (during nickel-affinity chromatography) using high concentrations of GHCl, followed by a gradual reduction in GHCl concentration to allow the protein to naturally refold into its unsaturated form. Refolded VC0430 retained the ability to bind substrate, as demonstrated by our thermal shift assays (see Results, 3.3.3.), and the viability of refolded protein preps was reaffirmed by the resemblance between their SEC traces (Fig. 11).

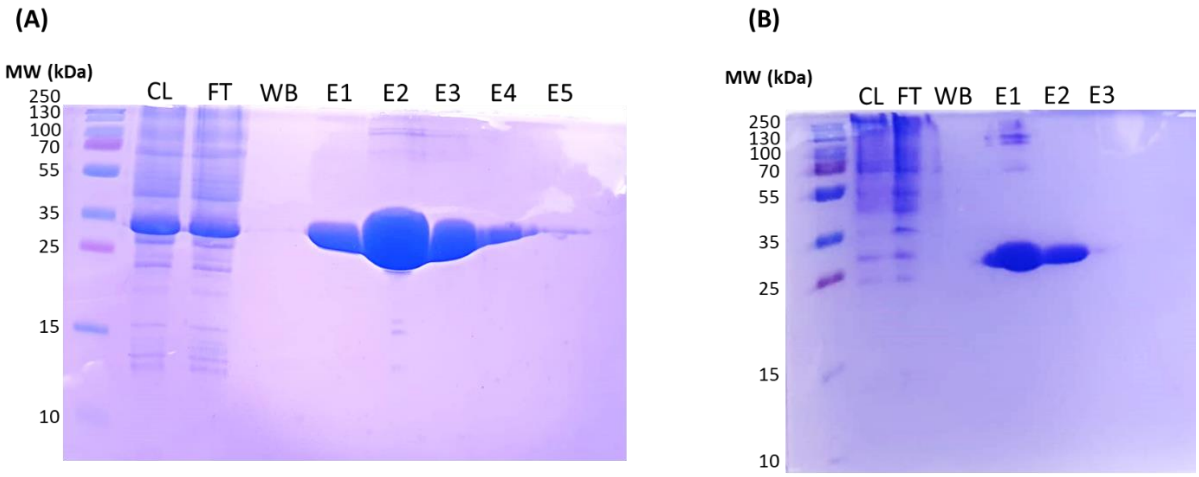

Figure 10. SDS-PAGE gels of VC0430 with (A) FLAG-His10-TEV tag and (B) C-terminal 6X-His-tag. Samples were collected after each purification step and loaded in the order as follows: molecular weight ladder; clarified lysate pre-purification (CL); clarified lysate after flowing through the nickel resin (FT); wash buffer after flowing through the nickel resin (WB); protein elutions (E1, E2, etc…). The eluted protein in both cases corresponded well to the estimated size of 35 kDa.

3.2.2. Size Exclusion Chromatography (SEC) of VC0430

SEC was performed to further purify protein preps after nickel-affinity chromatography. We were also able to assess the effect of refolding VC0430 by comparing SEC traces from refolded protein preps to traces of preps that had not previously been exposed to GHCl. SEC is a highly sensitive process, hence any detrimental changes to the structure of VC0430 as a result of the denaturation process could be characterized by a significant shift in the volume at which the protein elutes from the column, or any other obvious change to its SEC trace compared to the control (non-refolded VC0430). We observed no such changes to the result of SEC when each of these VC0430 preps were individually tested (Fig. 11A-B), suggesting that VC0430 can be benignly refolded as we previously described.

Purified VC0430 in SDS-PAGE gels (Fig. 10) was identified by one prominent band at around 30 kDa, suggesting that the free protein exists in a monomeric state. However, we aimed to use SEC to establish the oligomeric state of VC0430 when it is saturated with its substrate, as there has been past evidence to suggest that some TRAP SBPs, like TakP from *R. sphaeroides*, form dimers [1]. Evidence of the oligomeric state of saturated VC0430 would allow us to make preliminary predictions about how it contributes to the transport mechanism of this TAXI-TRAP system, whereby dimerization/oligomerization upon substrate-binding would refute our expectation that, like most other TRAP SBPs, VC0430 remains monomeric during this process.

The stage at which VC0430 was eluted from the column is shown by single peak at 16.79 mL which represents V_e (Fig. 11A). The addition of 1 mM glutamate to VC0430 (Fig. 11C), which

we had evidence binds VC0430 (see Results, 3.3.3.), had no significant effect on V_e or the overall SEC trace. It was therefore determined that the VC0430 remains in a monomeric state when interacting with its substrate, hinting that its role in transport could emulate that of the classical TRAP SBP, SiaP (from the SiaPQM system in *H. influenzae*) [24].

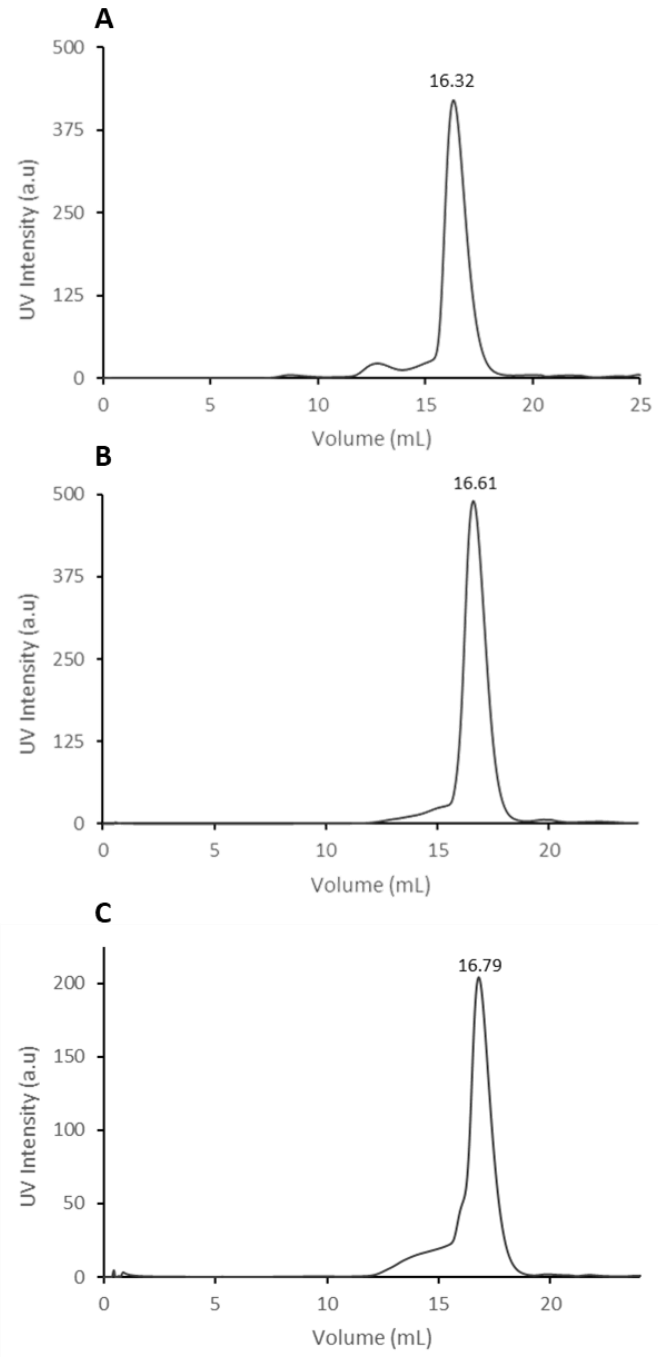

Figure 11. SEC traces for (A) non-refolded VC0430, (B) refolded VC0430 (C) refolded VC0430 with 1 mM glutamate. The similarity of traces (A) and (B) shows that refolding VC0430 has no substantial impact on its structure, reaffirming the viability of the protein to be used in subsequent assays. Further, (C) shows that the addition of glutamate to VC0430 before loading it on to the column made no significant difference to the outcome of SEC, thus indicating VC0430 remains monomeric upon binding to substrate.

Additionally, SEC was used to generate estimates for the molecular weight and Stoke's radius of VC0430; properties that provide some insight into the structural parameters of the protein whilst a crystal structure is yet to be determined. The molecular weight (kDa) and Stoke's radius (Å) of VC0430 were established through the generation of calibration curves using SEC standard proteins whose properties have already been characterized [50]. The procedure was carried out as described in the Materials & Methods section (Materials & Methods 2.4.2.), and the standard proteins used to form the calibration curves in this case were ferritin (440 kDa, 61 Å), ovalbumin (44 kDa, 30.5 Å), carbonic anhydrase (29 kDa, 23 Å) and ribonuclease A (13.7 kDa, 16.4 Å). As expected, these proteins eluted in order of size, with larger proteins coming off earlier than the smaller ones (Fig. 12A). To create the calibration curve for molecular weight, the K_{av} of each protein (see Materials and Methods, 2.4.2. for the formula) was plotted against the log of their molecular weight and a line of best fit was drawn through the data points. To determine the molecular weight of VC0430, the equation for K_{av} was applied and evaluation of the line of best fit gave a value of 28 kDa (Fig. 12B). The same principles were employed to devise a calibration curve for Stoke's radius, which gave a value of 23 Å for VC0430 (Fig. 12C).

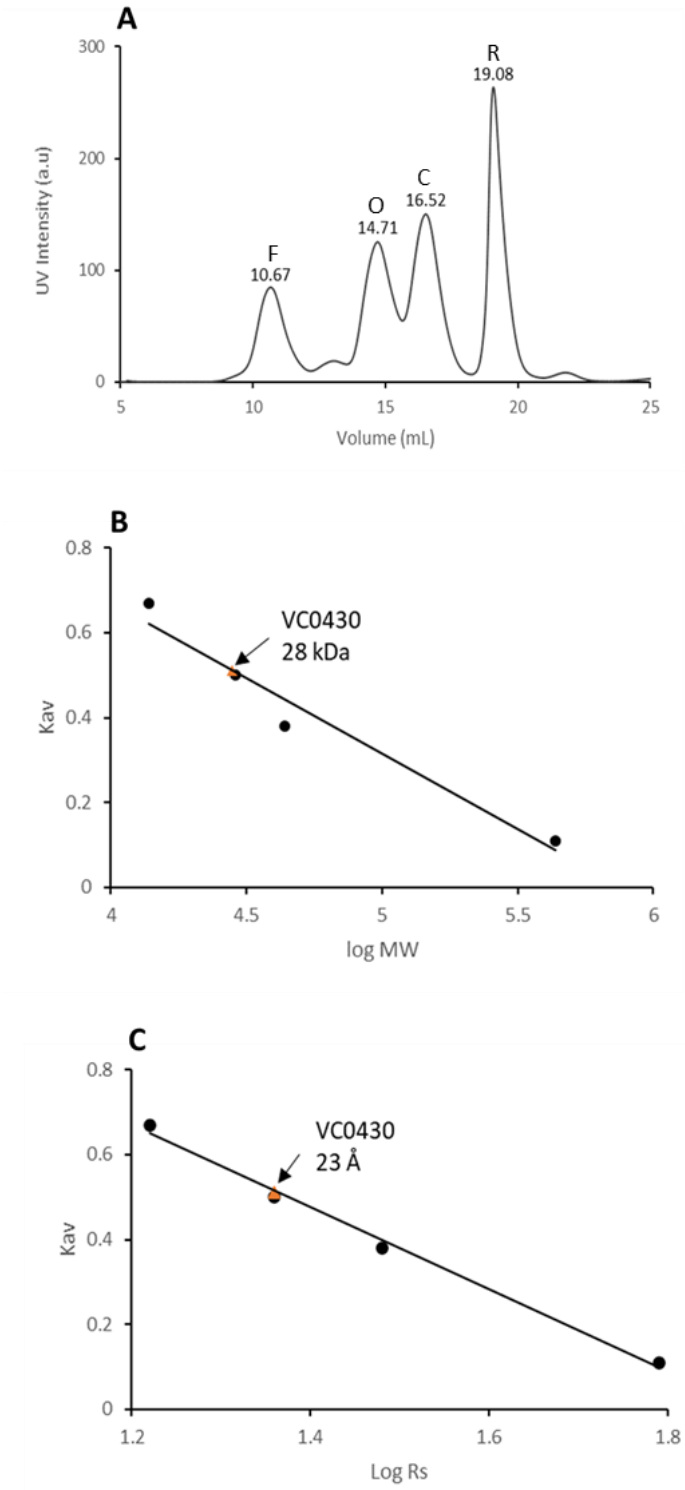

Figure 12. Determination of the molecular weight and Stoke's radius of VC0430 using SEC. (A) shows the SEC peaks for the standard proteins used to generate the calibration curves. Proteins eluted in order of size, whereby the first peak represents the largest protein- ferritin (F, 10.67 mL), followed by ovalbumin (O, 14.71 mL) and carbonic anhydrase (C, 16.52 mL), and finally ribonuclease A (R, 19.08 mL). The volume at which VC0430 is eluted, demonstrated by Fig. 11, is similar to that of carbonic anhydrase; hence why they share a similar K_{av}. (B) illustrates the estimate for the molecular weight of VC0430, which was 28 kDa, and (C) gives an estimated value of 23 Å for the Stoke's radius.

3.3. Screening Substrates for VC0430

3.3.1. Foundations and Optimisation of the Thermal Shift Assay

The thermal shift assay is a quick, temperature-based assay used to assess the stability of proteins by determining substrate-bound and non-substrate-bound melting temperatures. The method requires a small amount of protein and makes use of SYPRO orange dye, which binds to hydrophobic patches/denatured protein and fluoresces. As the temperature increases and the protein unfolds, fluorescence rises because the dye is increasingly able to bind hydrophobic patches as they become exposed, and this is monitored to determine a melting temperature (Tm) for the protein. Most proteins are stabilized by their substrates, therefore observing a significant increase in the temperature threshold at which the protein begins to unfold as a function of ligand concentration can serve as evidence of a direct interaction. Temperature and fluorescence monitoring is performed using a qPCR machine (real time PCR).

We aimed to perform a large-scale screen of different compounds in order to determine a substrate range for VC0430. However, before any substrates were screened, it was necessary to optimise the assay so that sufficient data could be produced. It was also essential that a standard Tm, in the absence of substrate, was determined for VC0430 so that binding-substrates could later be identified. The concentration of protein and buffer conditions that we used were influenced by previous literature. We found 5 µM of VC0430 in a 50 mM KPi pH 7.8 20 mM NaCl buffer to be adequate for these assays, though the concentration of SYPRO orange required to generate ample fluorescence needed to be established. Hence, various concentrations of dye were tested (Fig. 13), with 3.5x SYPRO producing the clearest trace with the least noise. This concentration was therefore used in all proceeding assays. The standard melting temperature for VC0430 was also determined to be an average of 63.38 °C.

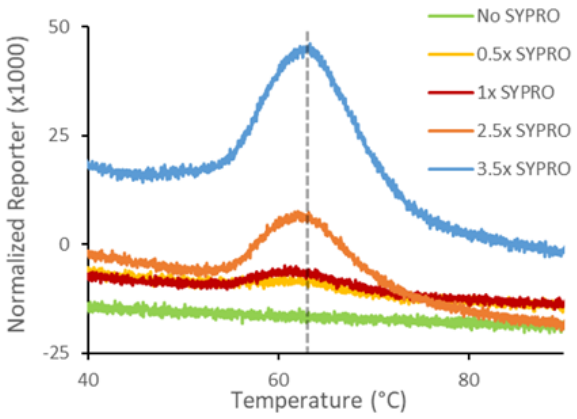

Figure 13. Optimisation of SYPRO concentration for the thermal shift assay. Increasing concentrations of SYPRO were tested to determine a suitable fluorescence intensity for assays. 3.5x SYPRO produced the clearest trace, so this was used in all future assays. Tm is indicated by the dashed line through the peak of the traces.

Throughout this report, data collected from thermal shift assays is illustrated in graphs displaying the normalized reporter against temperature. The normalized reporter is best described as 'the first derivative of the fluorescence emission as a function of temperature (−dF/dT)' [51], whereby the peak of a trace of -dF/dT vs temperature corresponds to the Tm of the protein. Here, we use dF/dT to accurately establish the Tm of VC0430, though it is also possible to determine the Tm from raw datasets through non-linear fitting of the fluorescence curve to the Boltzmann Equation (Fig. 14).

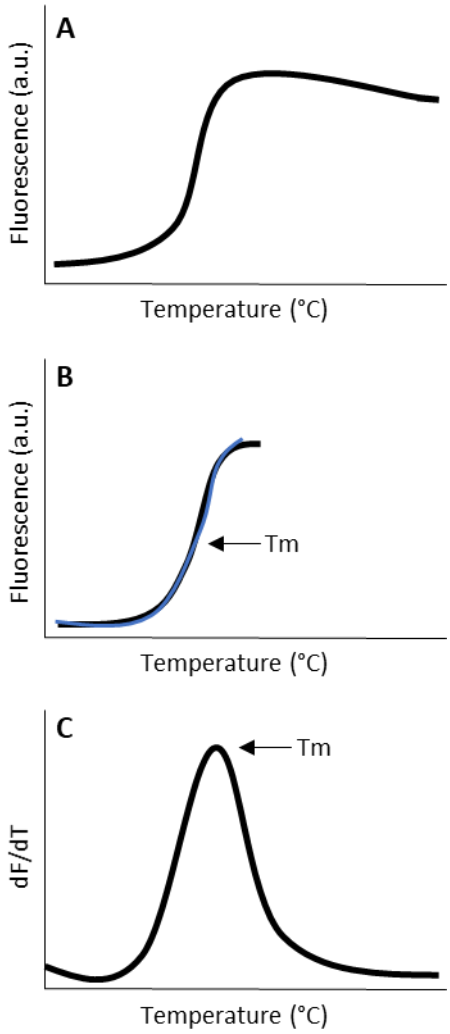

Figure 14. Graphic depiction of raw data and normalized data for the thermal shift assay. (A) An example of the raw denaturation trace of a protein; increasing temperature generates a sigmoidal fluorescence curve that represents the gradual denaturation of the protein. (B) Truncated denaturation trace that removes post-peak quenching due to protein-dye aggregation. The blue line is an example of a non-linear line of best fit that resembles the fitting of the fluorescence curve to the Boltzmann equation. (C) Normalized thermal shift trace that displays fluorescence as a function of temperature (dF/dT). Diagram adapted from [51].

3.3.2. Screening C4-Dicarboxylates with VC0430

The presence of MDH upstream to VC0430 in the same operon initially provided some reason to believe that VC0430 may bind to malate (see Results, 3.1.1.) and thus potentially some other C4-dicarboxylates. Additionally, a TAXI-TRAP SBP from *P. arcticus* was shown to be important for the growth of the microorganism on mineral media containing fumarate or butyrate [36], leading to the possibility that TAXI-TRAP SBPs, including VC0430, may be able to bind C4-dicarboxylates. We therefore attempted to biochemically assess whether this was the case for VC0430 using our thermal shift assays.

For all thermal shift assays, any substrate that improved the thermal stability of VC0430 by more than 2 °C was labelled a 'hit', as per the criteria set in the study of MatC from *R. palustris* [18]. Data for the screen of five different C4-dicarboxylates with VC0430 is displayed in Fig. 15, which shows that none of these substrates appear to bind the protein. Consequently, VC0430 was deemed unlikely to contribute to the transport of C4-dicarboxylates in *V. cholerae*.

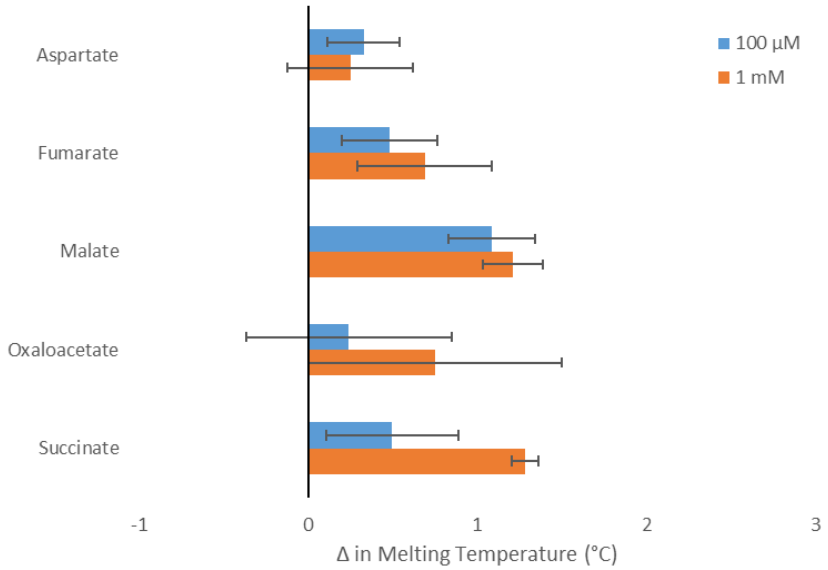

Figure 15. Thermal stability of VC0430 in the presence of C4-dicarboxylates. None of the C4-dicarboxylates screened caused a significant increase in the melting temperature of the protein, implying they do not bind. Each bar represents the mean Tm from technical triplicate datasets for each substrate, with the error bars showing the standard error of the mean. This experiment yielded the very similar results on two different occasions.

3.3.3. Screening C5- & C6-Dicarboxylates with VC0430

After providing evidence that VC0430 is not a C4-dicarboxylate binder, the logical next step was to further investigate the predictions made from our VC0430 homology model analysis (see Results, 3.1.3.), where it was hypothesized that, due to homology with the binding site of TtGluBP, VC0430 is a glutamate and glutamine binder. We looked to test this biochemically

by screening these substrates with VC0430 in the thermal shift assay. We also aimed to see if some other C5-dicarboxylates (along with glucose, a C6-dicarboxylate) bind the protein.

Fig. 16 shows that from the substrates screened, only glutamate, monosodium glutamate (MSG) and glutamine caused a substantial increase in the thermal stability of VC0430. Unsurprisingly given their likeness, glutamate and MSG triggered a similar increase in the Tm at both tested concentrations. At 100 µM, glutamate increased the Tm by 4.63 ± 0.25 °C whilst MSG increased it by 5.44 ± 0.15 °C, and at 1 mM the Tm increased by 8.03 ± 0.18 °C and 7.25 ± 0.35 °C for glutamate and MSG respectively. Glutamine caused a slightly smaller thermal shift at 100 µM (2.99 ± 0.38 °C) and 1 mM (4.64 ± 0.45°C) compared to the aforementioned binders. These findings confirmed the predictions made from the homology model and provides the first biochemically derived evidence of a substrate range for a TAXI-TRAP transporter.

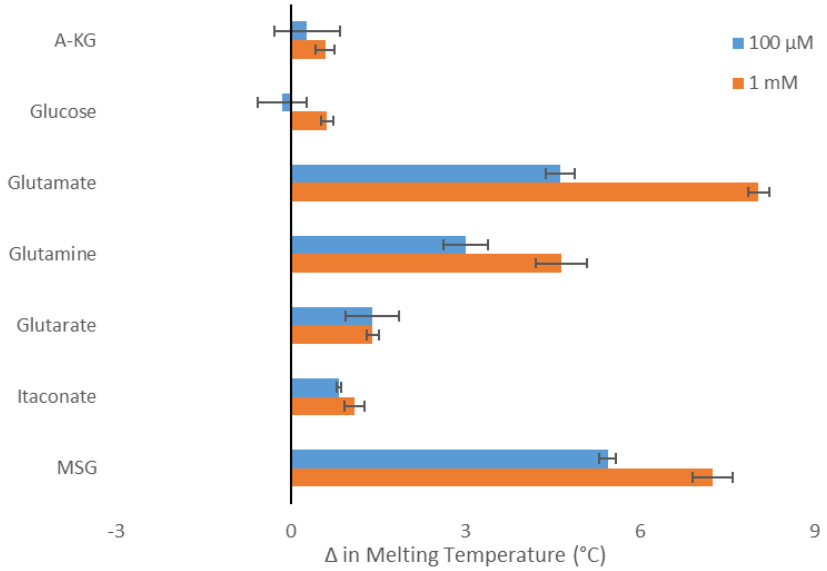

Figure 16. Thermal stability of VC0430 in the presence of C5- and C6-dicarboxylates. Of the substrates screened, glutamate, MSG and glutamine were the only ones that caused an increase in Tm of more than 2 °C for the protein. Each bar represents the mean Tm from technical triplicate datasets for each substrate, with the error bars showing the standard error of the mean. This experiment yielded the very similar results on two different occasions.

3.3.4. Screening the Remaining Amino Acids with VC0430

The binding of glutamine to VC0430 proved that the substrate range of the protein was not limited to dicarboxylic acids and opened the possibility for other amino acids to bind. Hence, all amino acids (excluding phenylalanine which was accidentally missed out) were screened to evaluate the specificity of the protein (Fig. 17). We found that none of these amino acids caused a significant increase in the Tm of the protein, suggesting that this TAXI-TRAP SBP in *V. cholerae* contributes solely to the binding of glutamate and glutamine.

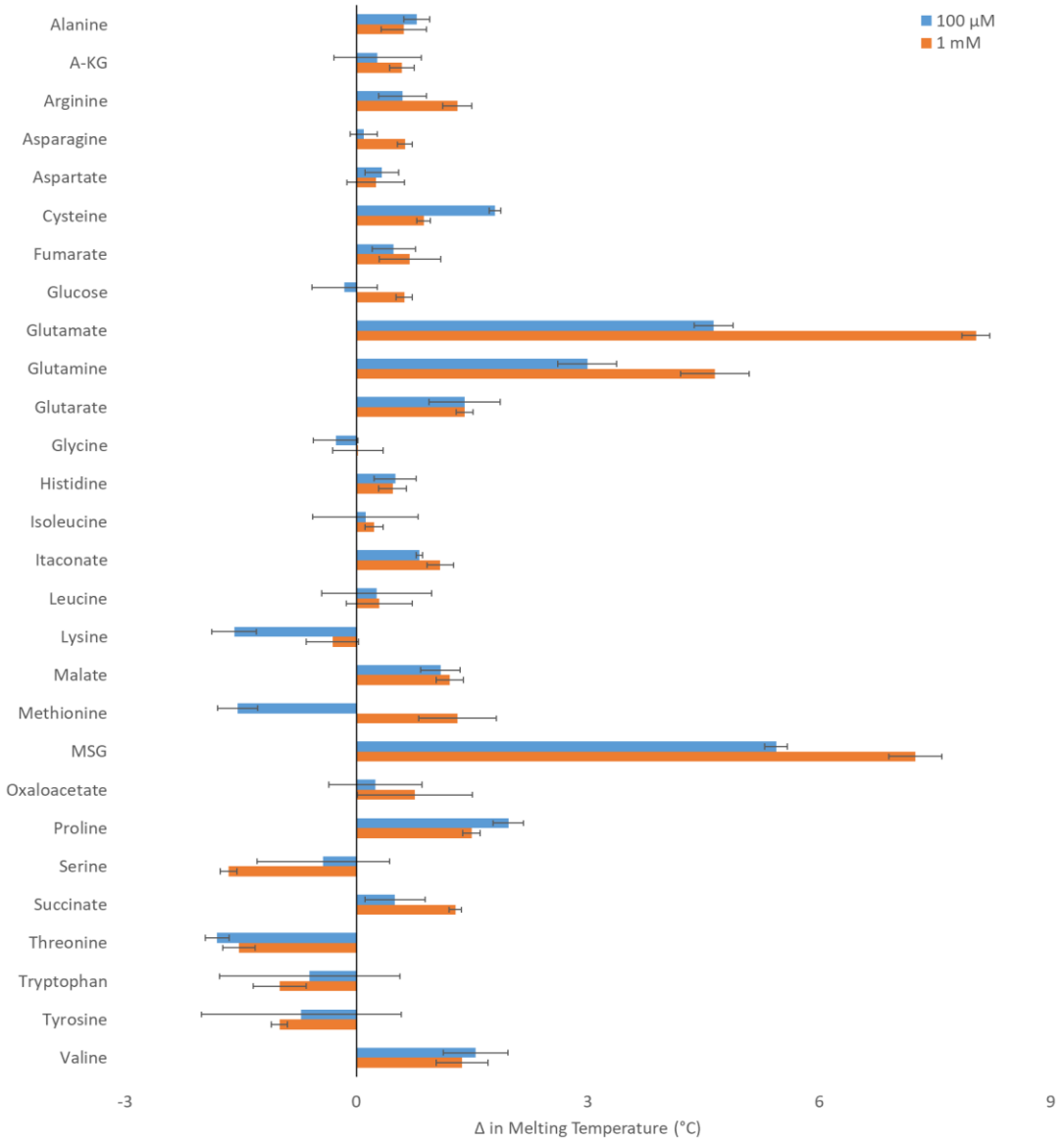

Figure 17. Thermal stability of VC0430 in the presence of all tested substrates. Apart from glutamate, MSG and glutamine, no significant increase in the thermal stability of VC0430 was observed for any of the other compounds screened, suggesting the SBP is highly specific. Each bar represents the mean Tm from technical triplicate datasets for each substrate, with the error bars showing the standard error of the mean. This experiment was performed on one, single occasion.

3.3.4. Effect of Reducing Agents on the Thermal Stability of VC0430

Analysis of the VC0430 homology model (Results, 3.1.3.) identified two pairs of cysteine residues on opposite sides of the structure. The two cysteines in each pair were predicted to form disulfide bridges between each other, leading to the expectation that these disulfide linkages may play a significant part in the overall stability of the protein. We aimed to explore this by observing how the presence of two different reducing agents, dithiothreitol (DTT) and tris(2-carboxyethyl)phosphine (TCEP), affects the stability of the protein in the thermal shift assay.

Preliminary attempts at exploring the effect of reducing agents on protein stability involved the use of 1 mM DTT under the same conditions used in substrate screening assays, except with the absence of substrate. Fig. 18A shows that DTT appears to have no effect on thermal stability, as there is no obvious change in the Tm compared to the reference. On initial assessment, this would appear to refute the presence of disulfides within overall structure of VC0430, however the more likely scenario is that DTT lost stability at a buffer pH of 7.8 [52] . TCEP, another widely used reducing agent, was used as alternative (at the same concentration, 1 mM) as it remains stable at a wider pH range and has been shown to be a more powerful reductant at pH values below 8.0 [52,53]. Consequently, TCEP was found to have shifted the Tm of VC0430 down from 63 °C to 59.97 ± 0.29 (Fig. 18B), suggesting that it breaks down the disulfide bonds present between the target cysteines in VC0430 and thus slightly reduces the overall stability of the protein. Unfortunately, the effect of TCEP on the binding ability of VC0430 was not determined, but we predict it is not likely to be detrimental as we purified pre-bound forms of VC0430 that had been expressed in the cytoplasm, which is a strong reducing environment.

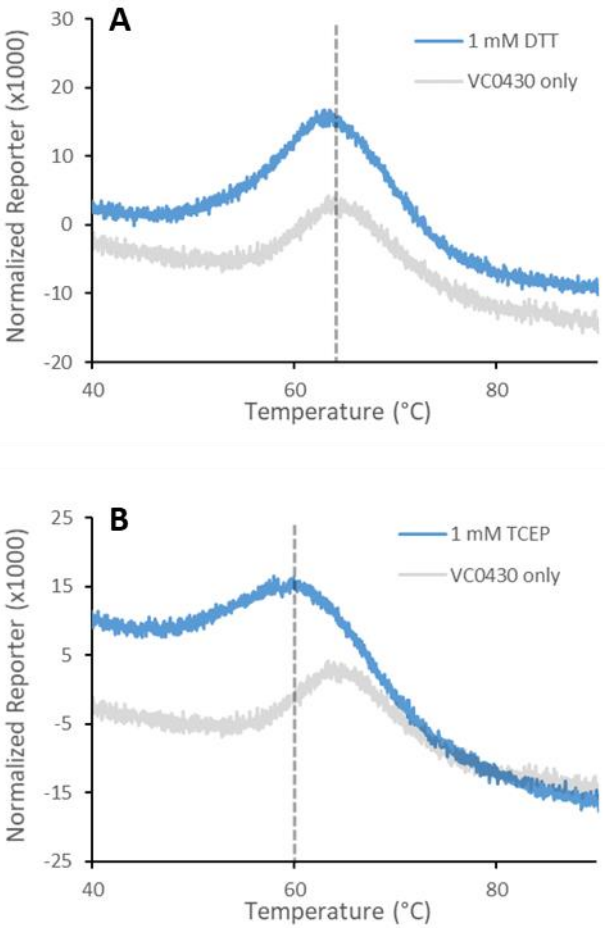

Figure 18. Effect of reducing agents on the stability of VC0430. Reducing agents are commonly used to break down disulfide bonds present within proteins. (A) shows that DTT has no effect on the thermal stability of VC030, however this likely due to it being incompatible with the pH of the assay buffer. (B) TCEP, a reducing agent that is less pH sensitive and generally more potent than DTT, causes a slight reduction in the thermal stability of VC0430, confirming the role of disulfides in the overall structure of the protein.

3.4. Intrinsic Tryptophan Fluorescence of VC0430

After data from our thermal shift assays established that VC0430 binds to both glutamate and glutamine, we attempted to use tryptophan fluorescence spectroscopy to determine the binding affinities of these substrates to the protein. Titrations of the change in tryptophan fluorescence were performed as described previously (Materials & Methods, 2.6.), but unfortunately regular inconsistencies in control titrations using known non-binders, including aspartate and malate, made performing this technique problematic. Fluorescence quenching was observed during titrations using glutamate, however there are some doubts over the accuracy of this data which will be further discussed shortly.

Before attempting any titrations, emission scans were performed using increasing concentrations of protein to establish the most suitable excitation and emission wavelengths to use in subsequent experiments. Fig 18A shows results from emission scan titrations at a range of 290-500 nm with a fixed excitation wavelength at 280 nm, which is the known excitation maximum for tryptophan [54]. We found that, in this case, tryptophan reaches its emission maximum at 330 nm, which matches its expected emission wavelength of around 350 nm [54]. Hence, for all future titration attempts, 280 nm and 330 nm were used as the values for the excitation and emission wavelengths, respectively.

Titrations using glutamate were performed as described in the Materials & Methods section (Materials & Methods, 2.6.). The concentration of glutamate added was gradually increased up to a maximum value of 2.1 µM, at which VC0430 appeared to be saturated (Fig. 19). The binding affinities from three technical repeats were used to estimate the K_d, which was determined to be 133 ± 53 nM after non-linear fitting of the data (Fig. 19B). Control titrations using known non-binders like aspartate, malate and glucose were always carried out before or after all attempts. On two separate occasions (including during the attempts seen in Fig. 19), these controls had no effect on the observed fluorescence values for VC0430, however, on 2 other occasions they caused quenching (see Appendix. 3). This caused uncertainty over the viability of the data seen in Fig. 19, and clearly, this assay needs further optimisation and repetition before our findings can be validated, but through our work here a starting point has been provided.

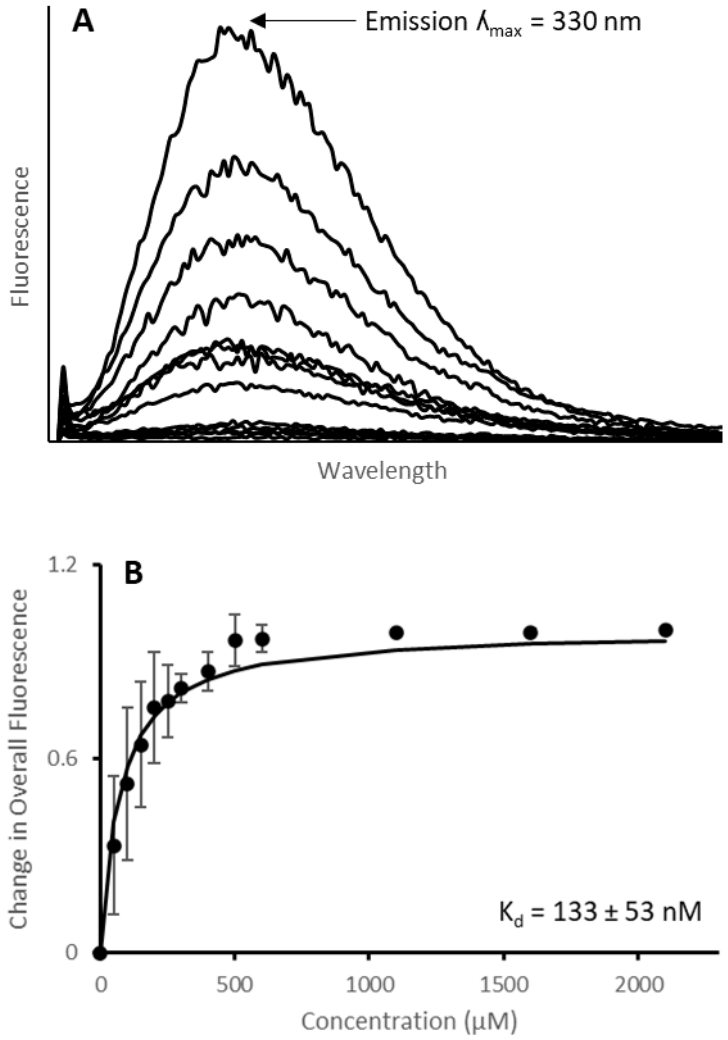

Figure 19. Fluorescence quenching enabled the prediction of the K_d between VC0430 and glutamate. (A) the emission scan results of fluorescence quenching when increasing concentrations of glutamate were added. The fluorescence peak was at a wavelength of 330 nm, verifying that it was indeed tryptophan fluorescence that was being observed. (B) Non-linear curve fitting of triplicate fluorescence quenching datasets enabled the prediction of a tight binding event between glutamate and VC0430, whereby the K_d was estimated to be 133 ± 53 nM. Datapoints are from one set of collected data, whereas error bars represent the standard deviation across triplicate datasets.

3.5. Microscale Thermophoresis Using VC0430

Microscale thermophoresis (MST) was trialled as an alternative binding assay to tryptophan fluorescence, with the hope that it could provide high resolution binding affinity data for VC0430 and its substrates. Despite its ability to produce very accurate data, the assay is very sensitive to various experimental conditions and the substrate itself can influence fluorescence readings generated by MST [55], making optimisation a challenging task. Although we were not able to establish a K_d for glutamate/glutamine binding to VC0430 using MST, we were able to determine the affinity of the dye (Second Generation RED-tris-NTA) to the protein and therefore provide a starting point for future attempts at this binding assay.

The principle of MST revolves around the change in thermophoresis of dyed protein molecules when they interact with substrate and undergo conformational changes [56]. Monitoring of this process is made possible by the fluorescence of the dye, whereby a binding event that changes the conformation of the dyed protein also alters the temperature dependence of the fluorescent dye, which is detected by the MST temperature jump [57]. Determining the K_d of the dye to VC0430 was necessary in order to establish the concentration of protein to be used for future experiments as well as the labelling efficiency of the protein. Fig. 20 shows the MST result of a 16-step titration series of protein samples (starting from 2 µM of VC0430) that were each mixed with 25 nM dye and suspended in 1X PBS-T buffer. The K_d of Second Generation RED-tris-NTA dye to VC0430 was determined to be 1.75 ± 0.11 nM, indicating high labelling efficiency, and also providing some validation of the compatibility of the dye for the protein.

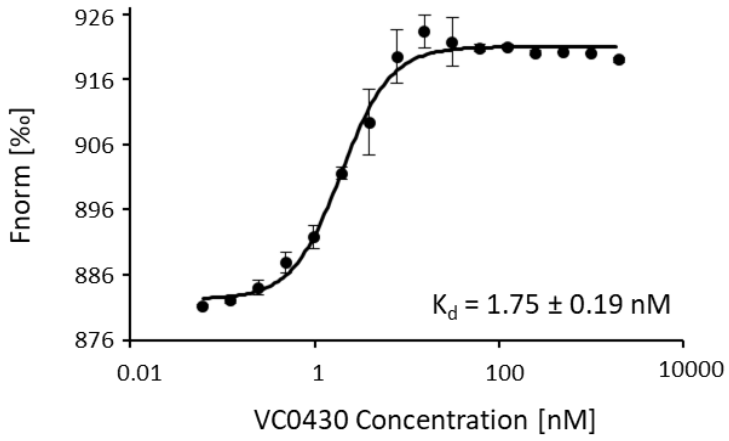

Figure 20. Characterization of VC0430 labelling with Second Generation RED-tris-NTA dye for MST. Tight association of the dye to VC0430 indicated a high labelling efficiency. This reinforces the suitability of Second Generation RED-tris-NTA to be used in future substrate-binding assays involving VC0430. Datapoints are from one set of collected data, whereas error bars represent the standard deviation across triplicate datasets.

CHAPTER 4: DISCUSSION

4.1. VC0430 as a TAXI-TRAP SBP

For the first time, a SBP from the TAXI-TRAP family of secondary membrane transporters has been biochemically characterized. Thermal shift assays described in this report provide evidence of VC0430 being a key component in a glutamate/glutamine membrane transportation system, thus offering further insight on past predictions made about the substrate range of TAXI-TRAP SBPs [1,35]. Data here highlights the ability of VC0430 to bind both glutamate and glutamine, confirming that VC0430, and almost certainly TtGluBP, are not mutually exclusive binders of each of these two substrates. Nevertheless, the fact that none of the other 30+ substrates screened in our thermal shift assays seemed to bind VC0430 suggests that this SBP is highly specific to its substrates. This is particularly evident when considering that neither glutarate, itaconate nor aspartate, all structurally very similar compounds to glutamate and glutamine, stimulated a binding event in our thermal shift assays.

As suggested above, a thorough comparison between the structures of glutamate/glutamine and some of the other compounds screened in our thermal shift assays provided some clues as to which components of VC0430 are involved in direct interactions with its substrates. For example, aspartate is a C4-dicarboxylate that is almost identical in structure to glutamate, however our data shows that it has no significant affinity for VC0430. This, along with the fact that no other shorter or longer length compounds increased the thermal stability of VC0430, suggests that the protein can only accommodate C5-carboxylates within its binding pocket. Taking that into consideration, our subsequent screening of two other structurally very similar C5-dicarboxylates to glutamate- glutarate and itaconate -showed that these substrates did not bind VC0430, suggesting that the protein is even more selective than originally presumed. Clearly, VC0430 is an amino acid binder, and conservation of Tyr32, Gln78, Glu111 from TtGluBP in VC0430 (Tyr45, Gln93 and Glu125, respectively) suggests that these residues have a specific involvement in stabilising the α-amino group of the substrate, as demonstrated by Takahashi *et al.* [35].

Among other factors, substrate binding events in VC0430 and TtGluBP are almost certainly dictated by the presence of carboxyl groups in both glutamate and glutamine. This is a feature that is homologous among classical TRAP SBPs, whereby a conserved arginine residue (Arg147 in SiaP from *H. influenzae*) coordinates the binding of carboxylic acids by forming a salt bridge with the carboxyl group of the substrate [1,33]. This residue, or something similar, was not conserved in our multiple sequence alignment of TAXI-TRAP SBPs, therefore hinting that some

members of this family may be able bind substrates even when carboxyl groups are absent. Characterization of other TAXI-TRAP SBPs would confirm whether this theory is correct, and, in this report, we have established numerous techniques and protocols which could be used to do this.

Through the use of homology modelling, a structure for VC0430 was generated. Although this is only a predictive model, we were still able to map its binding site to that of TtGluBP with a high degree of reliability, as per the good GMQE and QMEANDisCo scores, and provide supplementary evidence to our biochemical data that VC0430 is indeed a glutamate- and glutamine- binding protein. In their study of TtGluBP, Takahashi *et al.* identified many key binding site residues that had direct interactions with the bound substrate, whether that was glutamate or glutamine [35]. These residues are highly conserved within VC0430, and our structural model predicts that they inhabit a very similar composition to those within TtGluBP. This allows one to reasonably assume that the same interactions that occur between the substrate and the aforementioned residues in TtGluBP also occur within those that are conserved in VC0430. An example of this was suggested above when we considered the residues that are involved in stabilising the α-amino group of the substrate in both proteins [35]. Furthermore, by targeting the conserved residues that we have identified in VC0430, SDM can be used in future experiments to assess the influence that they have on the substrate-binding ability of the protein.

4.2. Significance of Glutamate & Glutamine for *V. cholerae*

4.2.1. The Role of Glutamate in Osmoadaptation

V. cholerae is a halophile that resides within the estuarine environment. Regular fluctuations in the ionic state and osmolarity of these aquatic ecosystems makes the survival of microorganisms a challenging task, however, *V. cholerae* has developed osmoadaptive mechanisms that facilitate its inhabitancy within its niche [58]. In their study of glutamate uptake levels in *V. cholerae*, Munro *et al.* found that uptake of this compound by the bacterium was significantly enhanced in high saline media, thus hinting at a role for glutamate in providing protection against changing osmotic pressures [59]. This was later expanded upon through gene knockout and NMR studies that explored the implication of ectoine synthesis on the survival of *V. cholerae* in different concentrations of NaCl [58]. Ectoine synthesis was shown to be induced by high-osmolarity, and the deletion of *ectA*, whose product is essential for generating ectoine, lead to decreased growth under increasing NaCl concentrations [58]. Nevertheless, supplementation of glutamate to wild-type *V. cholerae* cells under osmotic stress significantly increased growth, which is coherent with the fact that

glutamate is an essential substrate for ectoine synthesis [58,60]. This highlights a potential significant role for VC0430 in contributing to the delivery glutamate across the membrane so that it can be used for ectoine synthesis and hence osmoadaptation. An interesting and possibly very insightful future experiment to test the importance of VC0430 to this process would involve performing the experiments described above using Δ*vc0430* strains of *V. cholerae.*

4.2.2. Speculating the Importance of Glutamine to *V. cholerae*

Unlike glutamate, a specific role for glutamine in *V. cholerae* has not yet been characterized in literature. Despite being an obvious carbon source for the bacterium, the abundance of glutamine in seawater is not as high as some other amino acids [61], leading us to speculate that it does not have a specialized role in survival of *V. cholerae* within the estuarine environment like glutamate does. Nevertheless, glutamine is one of the most copious free amino acids found within the human body, and over a quarter of the total amount of glutamine in the body is utilized within the intestine [62]. With this considered, we hypothesize that the ability of VC0430 to bind and then deliver glutamine to the transport domains of the membrane could represent a unique adaptation that in some cases facilitates the survival of *V. cholerae* within the human intestine. This is emphasised by the role of glutamine within the bacterial cell, whereby it acts as an amino group donor for numerous biosynthetic reactions [63], including the reversible conversion of glutamine to glutamate by glutamate synthase [64]. This suggests a preliminary role for glutamine in the osmoadaptation of the bacterium.

4.3. VC0430 as a Potential Drug Target

It has previously been suggested that ectoine synthesis is very likely to also contribute to the survival of *V. cholerae* in the intestine [58]. The essential role that glutamate plays in ectoine synthesis clearly highlights VC0430 as a potential drug target in the treatment of cholera, since we have shown that it is a glutamate binding protein. The fact that VC0430 also binds glutamine, which can be used by bacteria and archaea to synthesise glutamate [64], suggests that inhibition of VC0430 could lead to significant loss of glutamate within the cell and therefore hinder the osmoadaptive abilities of *V. cholerae* within the intestine. How detrimental this would be to the bacterium depends on how many other glutamate/glutamine membrane transporters it possesses and how dependent it is on the overall TAXI-TRAP system that VC0430 belongs to. An obvious experiment that can be performed to characterize this involves comparing the growth of wild-type *V. cholerae* to Δ*vc0430* strains on glutamate- and/or glutamine- supplemented minimal media.

CHAPTER 5: CONCLUSION

The work carried out in this project aimed to provide novel insight into the TAXI-TRAP family of secondary membrane transporters by focussing in on a SBP, VC0430, from a TAXI-TRAP system in *V. cholerae*. We applied many different computational and *in vitro* techniques to characterize VC0430 and provide evidence of its substrate range. Using homology modelling, we accurately predicted the structure of the protein and identified key residues in the active site that are involved in the binding of glutamate or glutamine. This data was supported by the results from our thermal shift assays whereby, out of over 30+ substrates, only glutamate and glutamine increased the thermal stability of VC0430. Through our genome analysis and multiple sequence alignment, we also looked at the protein in the context of its local genetic neighbourhood as well as how homologous its genetic makeup is to numerous other TAXI-TRAP SBPs, thus providing a broader scope of the family as a whole. Further to this, we characterized the physical properties of the protein, including its molecular weight and Stoke's radius, and also explored the effect of reducing agents on its overall function.

Overall, this work has helped to provide a greater understanding of the TAXI-TRAP family of secondary membrane transporters; an area of which there has been very little previous research. We have considered the significance of our findings in the context of *V. cholerae* as both an organism adapting to survive in its environment as well as a pathogen to humans. Finally, we have demonstrated that our approach can be used to characterize other TAXI-TRAP SBPs, and we have also suggested future experiments that can be performed to further our knowledge of VC0430 as an essential component of a TAXI-TRAP transporter in *V. cholerae.*

REFERENCES

1 Mulligan, C., Fischer, M. and Thomas, G. H. (2011) Tripartite ATP-independent periplasmic (TRAP) transporters in bacteria and archaea. FEMS Microbiol. Rev. **35**, 68–86.

2 Tanaka, K. J., Song, S., Mason, K. and Pinkett, H. W. (2018) Selective substrate uptake: The role of ATP-binding cassette (ABC) importers in pathogenesis. Biochim. Biophys. Acta - Biomembr. **1860**, 868–877.

3 Maqbool, A., Horler, R. S. P., Muller, A., Wilkinson, A. J., Wilson, K. S. and Thomas, G. H. (2015) The substrate-binding protein in bacterial ABC transporters: Dissecting roles in the evolution of substrate specificity. Biochem. Soc. Trans. **43**, 1011–1017.

4 Forward, J. A., Behrendt, M. C., Wyborn, N. R., Cross, R. and Kelly, D. J. (1997) TRAP transporters: A new family of periplasmic solute transport systems encoded by the dctPQM genes of Rhodobacter capsulatus and by homologs in diverse gram-negative bacteria. J. Bacteriol. **179**, 5482–5493.

5 Rosa, L. T., Dix, S. R., Rafferty, J. B. and Kelly, D. J. (2017) Structural basis for high-affinity adipate binding to AdpC (RPA4515), an orphan periplasmic-binding protein from the tripartite tricarboxylate transporter (TTT) family in Rhodopseudomonas palustris. FEBS J. **284**, 4262–4277.

6 Peter, M. F., Gebhardt, C., Glaenzer, J., Schneberger, N., de Boer, M., Thomas, G. H., Cordes, T. and Hagelueken, G. (2021) Triggering Closure of a Sialic Acid TRAP Transporter Substrate Binding Protein through Binding of Natural or Artificial Substrates. J. Mol. Biol. **433**, 166756.

7 Rosa, L. T., Bianconi, M. E., Thomas, G. H. and Kelly, D. J. (2018) Tripartite ATP-independent periplasmic (TRAP) transporters and Tripartite Tricarboxylate Transporters (TTT): From uptake to pathogenicity. Front. Cell. Infect. Microbiol. **8**, 33.

8 De Boer, M., Gouridis, G., Vietrov, R., Begg, S. L., Schuurman-Wolters, G. K., Husada, F., Eleftheriadis, N., Poolman, B., McDevitt, C. A. and Cordes, T. (2019) Conformational and dynamic plasticity in substrate-binding proteins underlies selective transport in ABC importers. Elife 8:e44652.

9 Tang, C., Schwieters, C. D. and Clore, G. M. (2007) Open-to-closed transition in apo maltose-binding protein observed by paramagnetic NMR. Nature **449**, 1078–1082.

10 Gouridis, G., Schuurman-Wolters, G. K., Ploetz, E., Husada, F., Vietrov, R., De Boer, M., Cordes, T. and Poolman, B. (2015) Conformational dynamics in substrate-binding domains influences transport in the ABC importer GlnPQ. Nat. Struct. Mol. Biol. **22**, 57–64.

11 Herrou, J., Bompard, C., Antoine, R., Leroy, A., Rucktooa, P., Hot, D., Huvent, I., Locht, C., Villeret, V. and Jacob-Dubuisson, F. (2007) Structure-based Mechanism of Ligand Binding for Periplasmic Solute-binding Protein of the Bug Family. J. Mol. Biol. **373**, 954–964.

12 Herman, R., Bennett-Ness, C., Maqbool, A., Afzal, A., Leech, A. and Thomas, G. H. (2020) The salmonella enterica serovar typhimurium virulence factor STM3169 is a hexuronic acid binding protein component of a TRAP transporter. Microbiol. (United Kingdom) **166**, 284.

13 Chan, Y. C. and Wiedmann, M. (2009) Physiology and genetics of listeria monocytogenes survival and growth at cold temperatures. Crit. Rev. Food Sci. Nutr. **49**, 237–253.

14 Sweet, G. D., Somers, J. M. and Kay, W. W. (1979) Purification and properties of a citrate-binding transport component, the C protein of Salmonella typhimurium. Can. J. Biochem. **57**, 79–89.

15 Sweet, G. D., Kay, C. M. and Kay, W. W. (1984) Tricarboxylate-binding proteins of Salmonella typhimurium. Purification, crystallization, and physical properties. J. Biol. Chem. **259**, 1586–1592.

16 Huvent, I., Belrhali, H., Antoine, R., Bompard, C., Locht, C., Jacob-Dubuisson, F. and Villeret, V. (2006) Crystal structure of Bordetella pertussis BugD solute receptor unveils the basis of ligand binding in a new family of periplasmic binding proteins. J. Mol. Biol. **356**, 1014–1026.

17 Huvent, I., Locht, C., Belrhali, H., Antoine, R., Bompard, C., Jacob-Dubuisson, F. and Villeret, V. (2006) Structural analysis of Bordetella pertussis BugE solute receptor in a bound conformation. Acta Crystallogr. Sect. D Biol. Crystallogr. **62**, 1375–1381.

18 Rosa, L. T., Dix, S. R., Rafferty, J. B. and Kelly, D. J. (2019) A New Mechanism for High-Affinity Uptake of C4-Dicarboxylates in Bacteria Revealed by the Structure of Rhodopseudomonas palustris MatC (RPA3494), a Periplasmic Binding Protein of the Tripartite Tricarboxylate Transporter (TTT) Family. J. Mol. Biol. **431**, 351–367.

19 Shaw, J. G., Hamblin, M. J. and Kelly, D. J. (1991) Purification, characterization and nucleotide sequence of the periplasmic C4-dicarboxylate-binding protein (DctP) from Rhodobacter capsulatus. Mol. Microbiol. **5**, 3055–3062.

20 Walmsley, A. R., Shaw, J. G. and Kelly, D. J. (1992) The mechanism of ligand binding to the periplasmic C4-dicarboxylate binding protein (DctP) from Rhodobacter capsulatus. J. Biol. Chem. **267**, 8064–8072.

21 Rabus, R., Jack, D. L., Kelly, D. J. and Saier, M. H. (1999) TRAP transporters: An ancient family of extracytoplasmic solute-receptor-dependent secondary active transporters. Microbiology **145**, 3431–3445.

22 Kelly, D. J. and Thomas, G. H. (2001) The tripartite ATP-independent periplasmic (TRAP) transporters of bacteria and archaea. FEMS Microbiol. Rev. **25**, 405–424.

23 Mulligan, C., Kelly, D. J. and Thomas, G. H. (2007) Tripartite ATP-independent periplasmic transporters: Application of a relational database for genome-wide analysis of transporter gene frequency and organization. J. Mol. Microbiol. Biotechnol. **12**, 218–226.

24 Mulligan, C., Geertsma, E. R., Severi, E., Kelly, D. J., Poolman, B. and Thomas, G. H. (2009) The substrate-binding protein imposes directionality on an electrochemical sodium gradient-driven TRAP transporter. Proc. Natl. Acad. Sci. U. S. A. **106**, 1778–1783.

25 Fischer, M., Zhang, Q. Y., Hubbard, R. E. and Thomas, G. H. (2010) Caught in a TRAP: Substrate-binding proteins in secondary transport. Trends Microbiol. **18**, 471–478.

26 Allen, S., Zaleski, A., Johnston, J. W., Gibson, B. W. and Apicella, M. A. (2005) Novel sialic acid transporter of Haemophilus influenzae. Infect. Immun. **73**, 5291–5300.

27 Severi, E., Randle, G., Kivlin, P., Whitfield, K., Young, R., Moxon, R., Kelly, D., Hood, D. and Thomas, G. H. (2005) Sialic acid transport in Haemophilus influenzae is essential for lipopolysaccharide sialylation and serum resistance and is dependent on a novel tripartite ATP-independent periplasmic transporter. Mol. Microbiol. **58**, 1173–1185.

28 Jenkins, G. A., Figueira, M., Kumar, G. A., Sweetman, W. A., Makepeace, K., Pelton, S. I., Moxon, R. and Hood, D. W. (2010) Sialic acid mediated transcriptional modulation of a highly conserved sialometabolism gene cluster in Haemophilus influenzae and its effect on virulence. BMC Microbiol. **10**, 48.

29 Lubin, J. B., Kingston, J. J., Chowdhury, N. and Boyd, E. F. (2012) Sialic acid catabolism and transport gene clusters are lineage specific in Vibrio vulnificus. Appl. Environ. Microbiol. **78**, 3407–3015.

30 Steenbergen, S. M., Lichtensteiger, C. A., Caughlan, R., Garfinkle, J., Fuller, T. E. and Vimr, E. R. (2005) Sialic acid metabolism and systemic pasteurellosis. Infect. Immun. **73**, 1284–1294.

31 Thomas, G. H. (2016) Sialic acid acquisition in bacteria - one substrate, many transporters. Biochem. Soc. Trans. **44**, 760–765.

32 Müller, A., Severi, E., Mulligan, C., Watts, A. G., Kelly, D. J., Wilson, K. S., Wilkinson, A. J. and Thomas, G. H. (2006) Conservation of structure and mechanism in primary and secondary transporters exemplified by SiaP, a sialic acid binding virulence factor from Haemophilus influenzae. J. Biol. Chem. **281**, 22212–22222.

33 Fischer, M., Hopkins, A. P., Severi, E., Hawkhead, J., Bawdon, D., Watts, A. G., Hubbard, R. E. and Thomas, G. H. (2015) Tripartite ATP-independent Periplasmic (TRAP) Transporters use an arginine-mediated selectivity filter for high affinity substrate binding. J. Biol. Chem. **290**, 27113–27123.

34 Mayfield, J. E., Bricker, B. J., Godfrey, H., Crosby, R. M., Knight, D. J., Hailing, S. M., Balinsky, D. and Tabatabai, L. B. (1988) The cloning, expression, and nucleotide sequence of a gene coding for an immunogenic Brucella abortus protein. Gene **63**, 1–9.

35 Takahashi, H., Inagaki, E., Kuroishi, C. and Tahirov, T. H. (2004) Structure of the Thermus thermophilus putative periplasmic glutamate/glutamine-binding protein. Acta Crystallogr. Sect. D Biol. Crystallogr. **60**, 1846–1854.

36 Bakermans, C., Sloup, R. E., Zarka, D. G., Tiedje, J. M. and Thomashow, M. F. (2009) Development and use of genetic system to identify genes required for efficient low-temperature growth of Psychrobacter arcticus 273-4. Extremophiles **13**, 21–30.

37 Fernández, H., Prandoni, N., Fernández-Pascual, M., Fajardo, S., Morcillo, C., Díaz, E. and Carmona, M. (2014) Azoarcus sp. CIB, an anaerobic biodegrader of aromatic compounds shows an endophytic lifestyle. PLoS One **9**, e114955.

38 Sanz, D., García, J. L. and Díaz, E. (2020) Expanding the current knowledge and biotechnological applications of the oxygen-independent ortho-phthalate degradation pathway. Environ. Microbiol. **22**, 3478–3493.

39 Deka, R. K., Brautigam, C. A., Goldberg, M., Schuck, P., Tomchick, D. R. and Norgard, M. V. (2012) Structural, bioinformatic, and in vivo analyses of two treponema pallidum Lipoproteins reveal a unique TRAP transporter. J. Mol. Biol. **416**, 678–696.

40 Schapire, A. L., Valpuesta, V. and Botella, M. A. (2006) TPR proteins in plant hormone signaling. Plant Signal. Behav. **1**, 229–230.

41 Brautigam, C. A., Deka, R. K., Schuck, P., Tomchick, D. R. and Norgard, M. V. (2012) Structural and thermodynamic characterization of the interaction between two periplasmic Treponema pallidum lipoproteins that are components of a TPR-protein-associated TRAP transporter (TPAT). J. Mol. Biol. **420**, 70–86.

42 Vedadi, M., Niesen, F. H., Allali-Hassani, A., Fedorov, O. Y., Finerty, P. J., Wasney, G. A., Yeung, R., Arrowsmith, C., Ball, L. J., Berglund, H., et al. (2006) Chemical screening methods to identify ligands that promote protein stability, protein crystallization, and structure determination. Proc. Natl. Acad. Sci. U. S. A. **103**, 15835–15840.

43 Yammine, A., Gao, J. and Kwan, A. (2019) Tryptophan Fluorescence Quenching Assays for Measuring Protein-ligand Binding Affinities: Principles and a Practical Guide. BIO-PROTOCOL **9**, e3253.

44 Mulligan, C., Fenollar-Ferrer, C., Fitzgerald, G. A., Vergara-Jaque, A., Kaufmann, D., Li, Y., Forrest, L. R. and Mindell, J. A. (2016) The bacterial dicarboxylate transporter VcINDY uses a two-domain elevator-type mechanism. Nat. Struct. Mol. Biol.

45 Chowdhury, N., Norris, J., McAlister, E., Kathy Lau, S. Y., Thomas, G. H. and Fidelma Boyd, E. (2012) The

VC1777-VC1779 proteins are members of a sialic acid-specific subfamily of TRAP transporters (SiaPQM) and constitute the sole route of sialic acid uptake in the human pathogen Vibrio cholerae. Microbiol. (United Kingdom).

46 Biasini, M., Bienert, S., Waterhouse, A., Arnold, K., Studer, G., Schmidt, T., Kiefer, F., Cassarino, T. G., Bertoni, M., Bordoli, L., et al. (2014) SWISS-MODEL: Modelling protein tertiary and quaternary structure using evolutionary information. Nucleic Acids Res. **42**, 252–258.

47 Studer, G., Rempfer, C., Waterhouse, A. M., Gumienny, R., Haas, J. and Schwede, T. (2020) QMEANDisCo—distance constraints applied on model quality estimation. Bioinformatics **36**, 1765–1771.

48 Krachmarova, E., Tileva, M., Lilkova, E., Petkov, P., Maskos, K., Ilieva, N., Ivanov, I., Litov, L. and Nacheva, G. (2017) His-FLAG tag as a fusion partner of glycosylated human interferon-gamma and its mutant: Gain or loss? Biomed Res. Int. **2017**, 1–12.

49 Hopp, T. P., Prickett, K. S., Price, V. L., Libby, R. T., March, C. J., Cerretti, D. P., Urdal, D. L. and Conlon, P. J. (1988) A short polypeptide marker sequence useful for recombinant protein identification and purification. Bio/Technology **6**, 1204–1210.

50 Irvine, G. B. (2000) Determination of Molecular Size by Size-Exclusion Chromatography (Gel Filtration). Curr. Protoc. Cell Biol. **Chapter 5**, Unit 5.5.

51 Huynh, K. and Partch, C. L. (2016) Current Protocols in Protein Science: Analysis of protein stability and ligand interactions by thermal shift assay. Curr Protoc Protein Sci 79:28.9.1–28.9.14.

52 Getz, E. B., Xiao, M., Chakrabarty, T., Cooke, R. and Selvin, P. R. (1999) A comparison between the sulfhydryl reductants tris(2- carboxyethyl)phosphine and dithiothreitol for use in protein biochemistry. Anal. Biochem. **273**, 73–80.

53 Han, J. C. and Han, G. Y. (1994) A procedure for quantitative determination of tris(2-carboxyethyl)phosphine, an odorless reducing agent more stable and effective than dithiothreitol. Anal. Biochem. **220**, 5–10.

54 Möller, M. and Denicola, A. (2002) Protein tryptophan accessibility studied by fluorescence quenching. Biochem. Mol. Biol. Educ. **30**, 175–178.

55 Sparks, R. P. and Fratti, R. (2019) Use of microscale thermophoresis (MST) to measure binding affinities of components of the fusion machinery. Methods Mol. Biol. **1860**, 191–198.

56 Jerabek-Willemsen, M., André, T., Wanner, R., Roth, H. M., Duhr, S., Baaske, P. and Breitsprecher, D. (2014) MicroScale Thermophoresis: Interaction analysis and beyond. J. Mol. Struct. **1077**, 101–113.

57 Jerabek-Willemsen, M., Wienken, C. J., Braun, D., Baaske, P. and Duhr, S. (2011) Molecular interaction studies using microscale thermophoresis. Assay Drug Dev. Technol. **9**, 342–353.

58 Pflughoeft, K. J., Kierek, K. and Watnick, P. I. (2003) Role of Ectoine in Vibrio cholerae Osmoadaptation. Appl. Environ. Microbiol. **69**, 5919–5927.

59 Munro, P. M. and Gauthier, M. J. (1994) Uptake of glutamate by Vibrio cholerae in media of low and high osmolarity, and in seawater. Lett. Appl. Microbiol. **18**, 197–199.

60 Ono, H., Sawada, K., Khunajakr, N., Tao, T., Yamamoto, M., Hiramoto, M., Shinmyo, A., Takano, M. and Murooka, Y. (1999) Characterization of biosynthetic enzymes for ectoine as a compatible solute in a moderately halophilic eubacterium, Halomonas elongata. J. Bacteriol. **181**, 91–99.

61 Dawson, R. and Liebezeit, G. (1981) THE ANALYTICAL METHODS FOR THE CHARACTERISATION OF

ORGANICS IN SEAWATER. Mar. Org. Chem. **31**, 445–496.

62 Kim, M. H. and Kim, H. (2017) The roles of glutamine in the intestine and its implication in intestinal diseases. Int. J. Mol. Sci. **18**, 1051.

63 Braunstein, A. E. and Hsu Ting Seng. (1960) The scope of amino donor specificity of glutamine transaminase and asparagine transaminase. BBA - Biochim. Biophys. Acta **44**, 187–189.

64 Jongsareejit, B., Rahman, R. N. Z. A., Fujiwara, S. and Imanaka, T. (1997) Gene cloning, sequencing and enzymatic properties of glutamate synthase from the hyperthermophilic archaeon Pyrococcus sp. KOD1. Mol. Gen. Genet. **254**, 635–642.

APPENDIX

Appendix. 1

Individual thermal shift traces for all substrates screened with VC0430 in thermal shift assays.

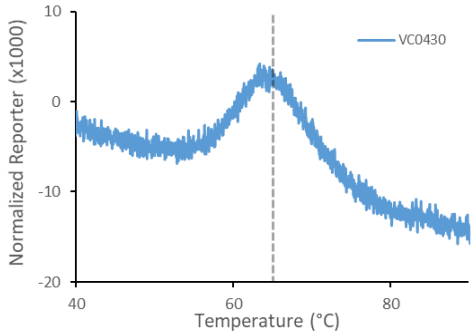

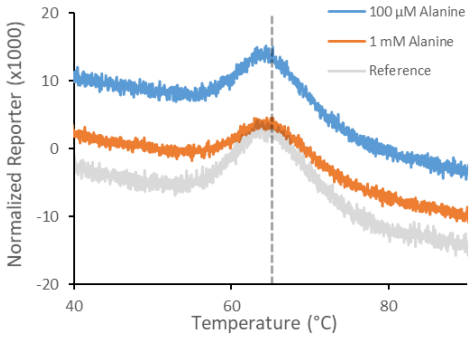

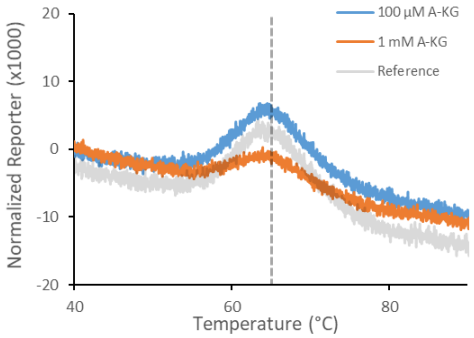

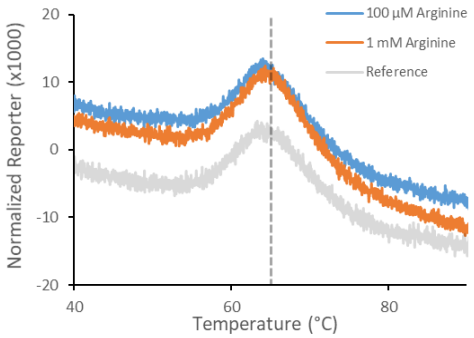

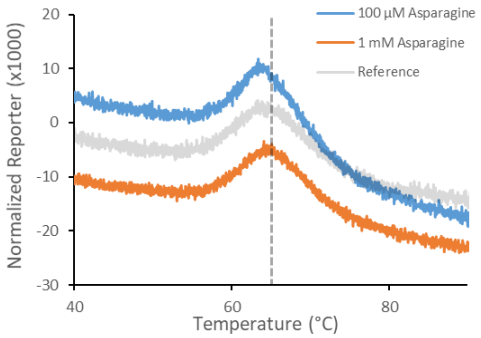

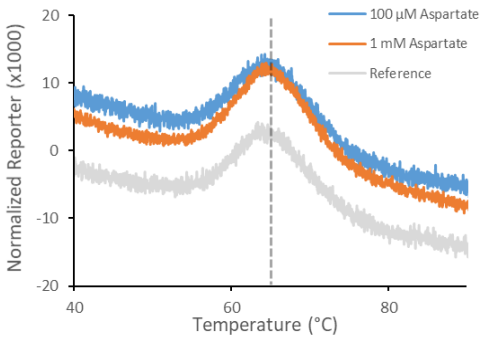

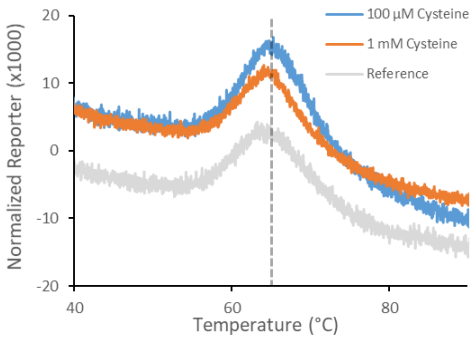

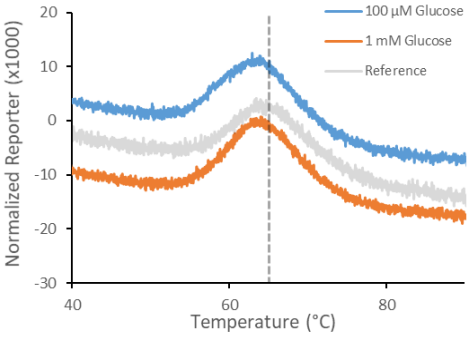
100 µM Glucose
1 mM Glucose
Reference
Normalized Reporter (x1000)
Temperature (°C)

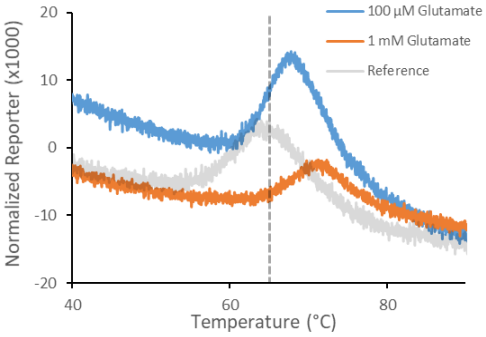
100 µM Glutamate
1 mM Glutamate
Reference
Normalized Reporter (x1000)
Temperature (°C)

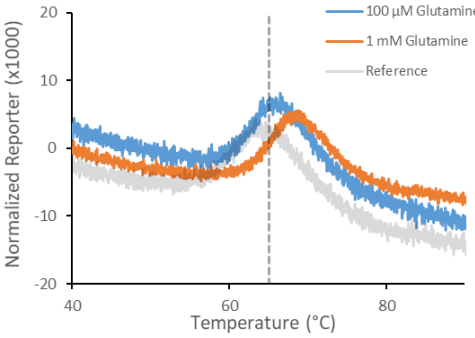
100 µM Glutamine
1 mM Glutamine
Reference
Normalized Reporter (x1000)
Temperature (°C)

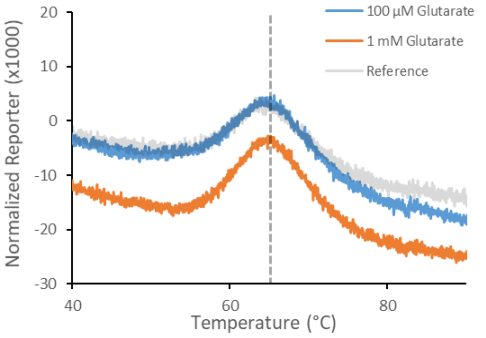
100 µM Glutarate
1 mM Glutarate
Reference
Normalized Reporter (x1000)
Temperature (°C)

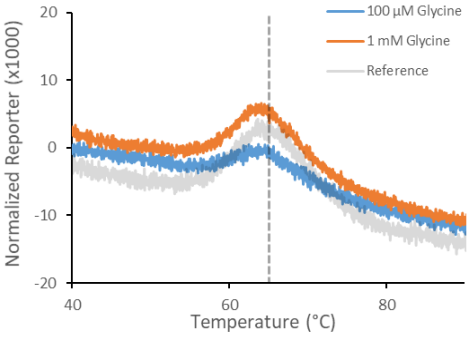
100 µM Glycine
1 mM Glycine
Reference
Normalized Reporter (x1000)
Temperature (°C)

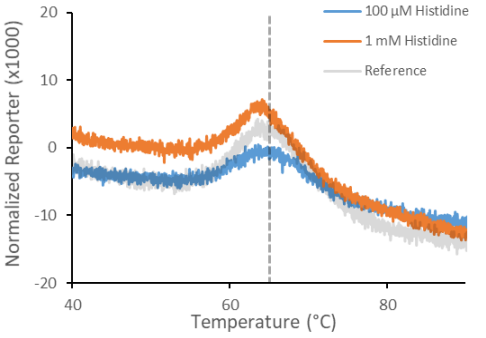
100 µM Histidine
1 mM Histidine
Reference
Normalized Reporter (x1000)
Temperature (°C)

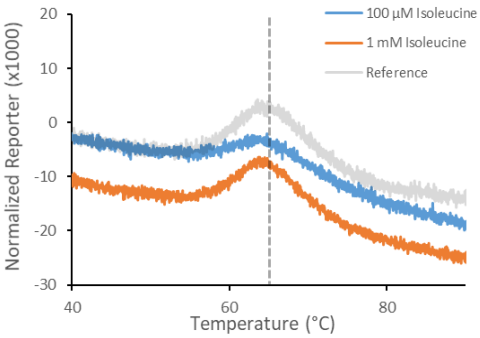
100 µM Isoleucine
1 mM Isoleucine
Reference
Normalized Reporter (x1000)
Temperature (°C)

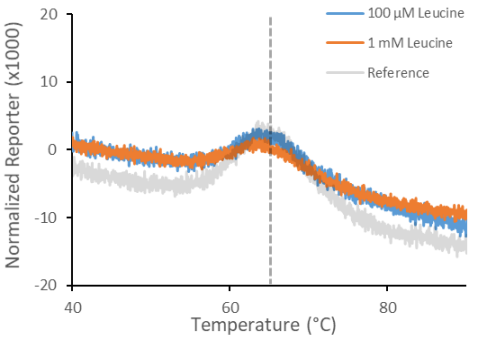
100 µM Leucine
1 mM Leucine
Reference
Normalized Reporter (x1000)
Temperature (°C)

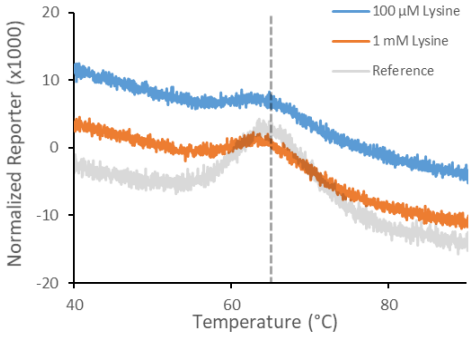
100 µM Lysine
1 mM Lysine
Reference
Normalized Reporter (x1000)
Temperature (°C)

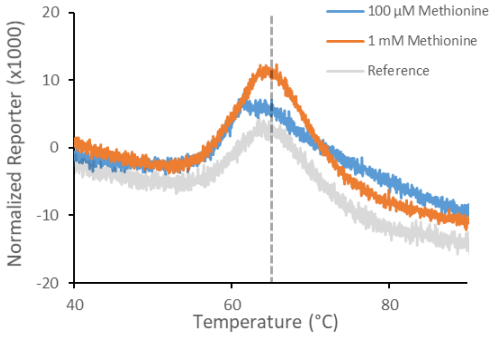
100 µM Methionine
1 mM Methionine
Reference
Normalized Reporter (x1000)
Temperature (°C)

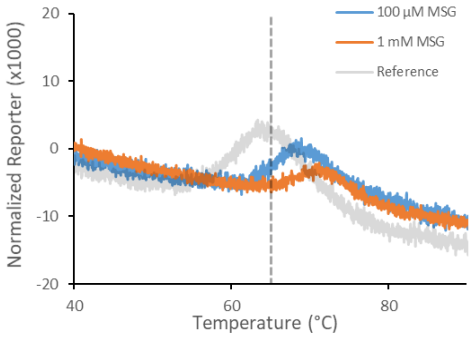
100 µM MSG
1 mM MSG
Reference
Normalized Reporter (x1000)
Temperature (°C)

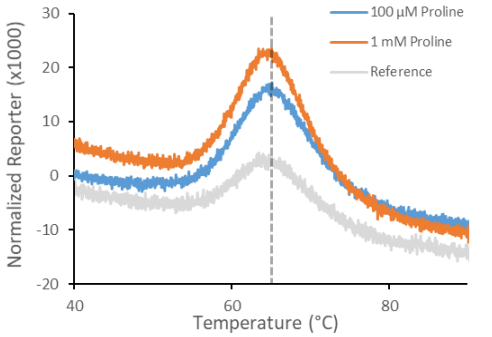
100 µM Proline
1 mM Proline
Reference
Normalized Reporter (x1000)
Temperature (°C)

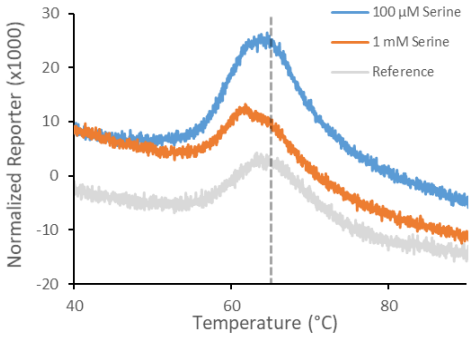
100 µM Serine
1 mM Serine
Reference
Normalized Reporter (x1000)
Temperature (°C)

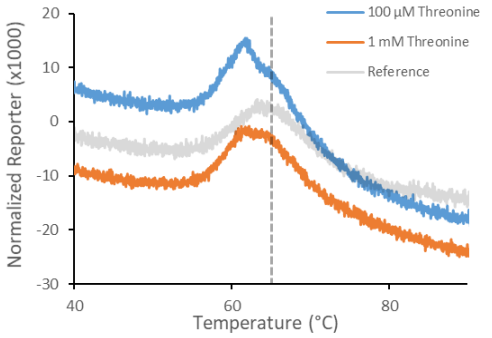
100 µM Threonine
1 mM Threonine
Reference
Normalized Reporter (x1000)
Temperature (°C)

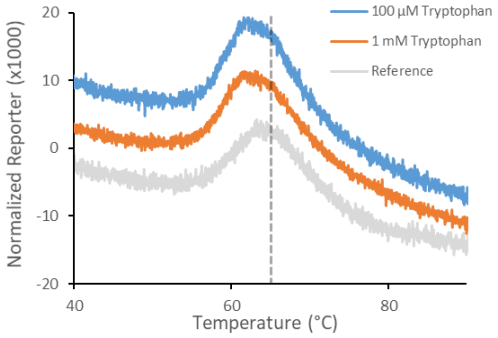
100 µM Tryptophan
1 mM Tryptophan
Reference
Normalized Reporter (x1000)
Temperature (°C)

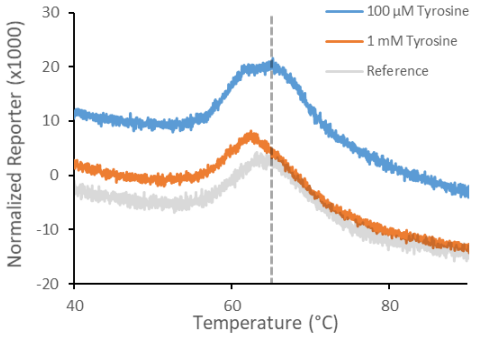
100 µM Tyrosine
1 mM Tyrosine
Reference
Normalized Reporter (x1000)
Temperature (°C)

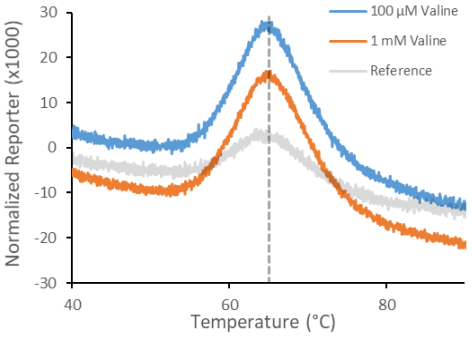
100 µM Valine
1 mM Valine
Reference
Normalized Reporter (x1000)
Temperature (°C)

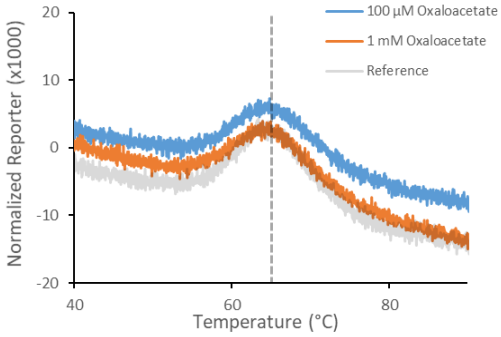
100 µM Oxaloacetate
1 mM Oxaloacetate
Reference
Normalized Reporter (x1000)
Temperature (°C)

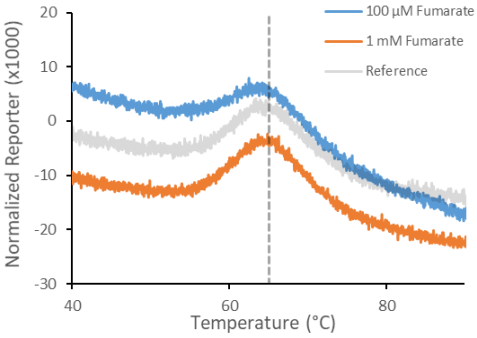
100 µM Fumarate
1 mM Fumarate
Reference
Normalized Reporter (x1000)
Temperature (°C)

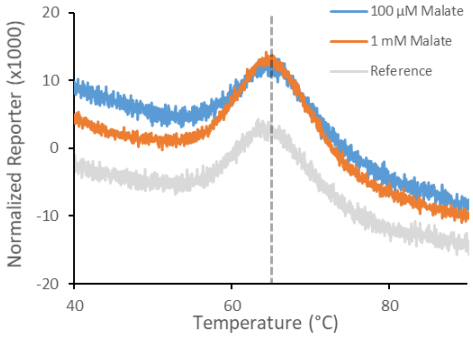
100 µM Malate
1 mM Malate
Reference
Normalized Reporter (x1000)
Temperature (°C)

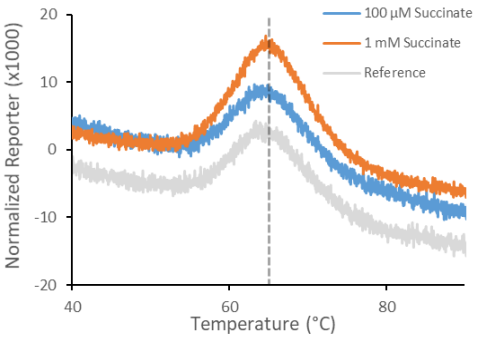
100 µM Succinate
1 mM Succinate
Reference
Normalized Reporter (x1000)
Temperature (°C)

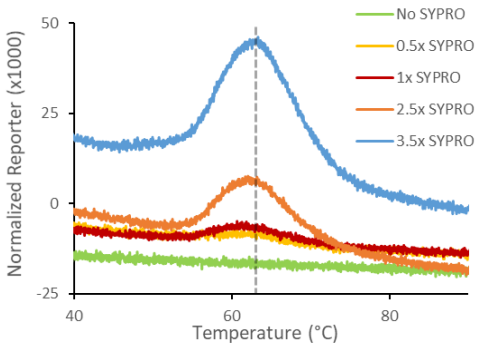
No SYPRO
0.5x SYPRO
1x SYPRO
2.5x SYPRO
3.5x SYPRO
Normalized Reporter (x1000)
Temperature (°C)

Appendix. 2

Traces of occasions when malate and aspartate (controls) caused quenching during tryptophan fluorescence spectroscopy, leading to doubts over glutamate titration data.